

Part I

Non-Ionizing Radiation

1

Sub-Terahertz Radiation Including Radiofrequency (RF) and Microwave Radiation

1.1

Absorption

1.1.1

General Aspects

The regime of the electromagnetic spectrum corresponding to frequencies lower than $1 \text{ THz} = 10^{12} \text{ Hz}$ – that is, to photon energies lower than that of infrared (IR) light – is commonly divided into three sections: (i) the sub-radiofrequency (RF) region, ranging from 10^{-6} Hz to $3 \times 10^3 \text{ Hz}$; (ii) the RF region, ranging from $3 \times 10^3 \text{ Hz}$ to $3 \times 10^8 \text{ Hz}$ (1.24×10^{-11} to $1.24 \times 10^{-6} \text{ eV}$, corresponding to wavelengths *in vacuo* of 10^5 to 1 m); and (iii) the microwave region, ranging from $3 \times 10^8 \text{ Hz}$ to $3 \times 10^{11} \text{ Hz}$ (1.24×10^{-6} to $1.24 \times 10^{-3} \text{ eV}$, corresponding to wavelengths *in vacuo* of 1 m to 10^{-3} m). Both, RF and microwave radiation are widely used for all types of telecommunication techniques, including radio, television, wireless telephoning, and radar (radio detection and ranging), and therefore the use of these electromagnetic waves is regulated by government agencies. In many countries, the frequencies 0.869, 0.915 and 2.45 GHz, corresponding to $\lambda = 0.345 \text{ m}$, 0.328 m and 0.122 m , respectively, are provided for industrial and private usage. Commonly, domestic microwave ovens are operated at 2.45 GHz.

Basically, the absorption of the various types of sub-THz radiation follows the same principle, and therefore its treatise will be coupled together here. The photon energy of sub-THz radiation is lower than about 10^{-3} eV , and thus at least about three orders of magnitude lower than the binding energies of atoms in molecules. This implies that chemical reactions cannot be induced directly by single photons of these radiations. However, if sub-THz radiation is absorbed, heat will be generated – that is, photon energy will be converted into translational energy. The phenomenon related to the fact that the absorption of sub-THz radiation results in heating is commonly referred to as *dielectric loss heating*. The resultant increase in temperature can be the cause of the initiation or acceleration of chemical reactions. Now, the question arises: How is photon energy converted into translational energy in this case? Actually, only polar materials consisting of molecules with a

permanent dipole moment and materials containing mobile ions are capable of absorbing sub-THz radiation, whereas nonpolar materials are almost transparent. This explains why polar polymers such as poly(methyl methacrylate) and poly(vinyl acetate) are absorbing, but nonpolar polymers such as polyethylene, polypropylene and polytetrafluoroethylene are nonabsorbing materials. According to a model originating from P. Debye [1,2] (who received the Nobel Prize in Chemistry in 1936), sub-THz radiation interacts with nonionic systems containing polar entities via *orientation polarization* of the permanent dipoles; that is, the dipole moments tend to align parallel to the direction of the external electric field, provided that the mobility of the polar entities is sufficiently high. At relatively low frequencies, the dipoles have ample time to follow the variations of an external alternating electric field. However, as the frequency increases, the dipoles are unable to fully restore their original positions during field reversals; that is, the dipolar reorientation lags behind the applied field and eventually stops. Energy is absorbed by the system, as long as electric field-enforced motions of the polar entities take place.

The phenomenon of orientation polarization under the influence of an outer alternating electric field is referred to as *dielectric relaxation*. Relaxation, in its original meaning, relates to the re-establishment of an equilibrium state of a system that has been distorted by an outer force. In a frequently used broader sense, the term relaxation relates to the ability of a system to undergo distortions under the influence of an outer force. In the present case, the motions of polar groups contained in a system in the condensed state are enforced by an outer electric field; that is, dipole vectors orient themselves with respect to the direction of the outer electric field. In this sense, dielectric relaxation resembles mechanical relaxation involving strain release after strain build-up. The relaxation of a system is characterized by the relaxation time τ , which, generally speaking, corresponds to the time that the system needs to return to the equilibrium state after distortion by an outer force. With respect to polar groups being exposed to an outer electric field, τ characterizes their mobility and, in an extrapolated sense, the mobility of the whole system. The extent of energy absorption is essentially determined by the magnitude of the relaxation time τ (see Section 1.1.2.1). In the case of polymers, the determination of relaxation times is an important feature of dielectric spectroscopy (see Section 1.3.1).

The radiation-induced orientation polarization of dipolar molecules or groups consumes energy on a molecular scale (internally dissipated as heat) to overcome internal constraints induced by the external electric field. Electrically nonconducting materials capable of undergoing dielectric relaxation are commonly denoted as *dielectrics*.

In systems containing mobile charge carriers, another mechanism of energy absorption becomes operative. Here, electromagnetic waves induce an electric current which generates heat. In this context it is notable that microwave absorption can serve as a tool to detect charge carriers; for example, a characteristic microwave absorption signal can be detected (see Section 1.3.2) when charge carriers are generated in a nonconducting medium upon irradiation with a pulse of ultraviolet (UV) laser light.

In heterogeneous dielectric systems comprising small fractions of electrically conducting phases, another mode of polarization arises from the charge build-up in *interfaces* between chemically different components, termed *interfacial* (space charge) or *Maxwell–Wagner polarization*. Both, orientation and interfacial polarization are the basis for energy absorption in many industrial materials subjected to alternating electric fields during processing.

1.1.2

Dissipation of Energy

The parameter characterizing the interaction of sub-THz radiation with matter is the complex relative dielectric constant ε (dimensionless), also called complex permittivity (Equation 1.1).

$$\varepsilon = \varepsilon' - j \varepsilon'' \quad (1.1)$$

Here, $j = \sqrt{-1}$. The term *relative* means relative to free space (*in vacuo*). Absolute values are obtained according to Equation 1.2 by multiplying ε with the permittivity of free space $\varepsilon_0 = 8.85 \times 10^{-12} \text{ F m}^{-1}$.

$$\varepsilon_{\text{abs}} = \varepsilon \varepsilon_0 = (\varepsilon' - j \varepsilon'') \varepsilon_0 \quad (\text{F m}^{-1}) \quad (1.2)$$

The real part ε' of the complex dielectric constant relates to the energy reversibly stored and released per cycle of the alternating field; that is, ε' characterizes the ability of the irradiated material to be polarized and to propagate the wave. The imaginary part $-j\varepsilon''$ relates to the energy absorbed per cycle; that is, ε'' , which is also called the *loss factor*, characterizes the ability of the irradiated material to absorb (dissipate) energy – that is, to convert sub-THz energy quanta into heat. Frequently, the *dielectric performance* of materials is characterized by the ratio of ε'' to ε' , denoted as $\tan \delta = \varepsilon''/\varepsilon'$. Polar materials contain a large number of permanent dipoles which all contribute to the loss factor. The latter is obtained experimentally and commonly denoted as the *effective loss factor* (for the sake of simplicity, the attribute *effective* is omitted in the following text). The dielectric properties of typical nonpolar and polar polymers are listed in Tables 1.1 and 1.2, respectively. Both ε' and ε'' vary with frequency and temperature.

1.1.2.1 Frequency Dependence

$\varepsilon(\omega)$, the complex dielectric function of a material, can be obtained by measuring the capacitance C_0 and C of a capacitor in the absence and presence of the material, respectively, with the aid of Equation 1.3:

$$\varepsilon(\omega) = \frac{C}{C_0} \quad (1.3)$$

By using a sinusoidal electric field $E(\omega) = E_0 \exp(j\omega t)$ with an angular frequency $\omega = 2\pi\nu$, the complex permittivity can be obtained by measuring the complex

Table 1.1 Dielectric properties of nonpolar polymers at 20 to 30 °C [3,7].

Polymer	Frequency (Hz)	ϵ' ^{a)}	ϵ'' ^{b)}
Polypropylene	10^3	2.4	$<1.2 \times 10^{-3}$
	10^5	2.4	$<1.2 \times 10^{-3}$
	10^7	2.4	$<(1.2-4.5) \times 10^{-3}$
	10^9	2.4	
Butadiene-styrene rubber	10^4	2.5	2.5×10^{-3}
	10^5	2.5	4.5×10^{-3}
	10^7	2.5	16.9×10^{-3}
	10^9	2.5	10.8×10^{-3}
Hevea rubber	10^4	2.4	3.4×10^{-3}
	10^5	2.4	3.4×10^{-3}
	10^7	2.4	7.7×10^{-3}
	10^8	2.2	12.0×10^{-3}
	10^9		6.4×10^{-3}
Polystyrene	10^3	2.5	4×10^{-3}
	10^9	2.5	4×10^{-3}
Poly(tetrafluoroethylene-co-hexa-fluoropropene) (90:10, w/w)	10^5	2.1	0.5×10^{-3}
	10^7	2.1	1.0×10^{-3}
	10^9	2.1	2.3×10^{-3}
	10^{10}	2.1	1.5×10^{-3}

a) Real part of the complex relative dielectric constant.

b) Loss factor.

Table 1.2 Dielectric properties of polar polymers at 20 to 30 °C [3].

Polymer	Frequency (Hz)	ϵ' ^{a)}	ϵ'' ^{b)}
Polychloroprene (1,4-poly(2-chloro-1,3-butadiene))	10^4	6.2	0.205
	10^5	6.1	0.183
	10^7	4.7	0.940
	10^9	2.84	0.136
Poly(methyl methacrylate)	10^4	3.0	0.100
	10^5	2.9	0.082
	10^7	2.8	0.048
	10^8	2.7	0.032
Poly(ethylene terephthalate)	10^3	3.3	0.016
	10^6	2.4	0.048
	10^9	2.4	0.008
Polyamide-6	10^3	3.5	0.035
	10^5	3.4	0.065
	10^7	3.2	0.096
	10^9	3.1	0.062
Cellulose	10^3	7.2	0.145
	10^4	7.0	0.21
	10^7	5.8	0.46
	10^8	5.6	0.39

a) Real part of the complex relative dielectric constant.

b) Loss factor.

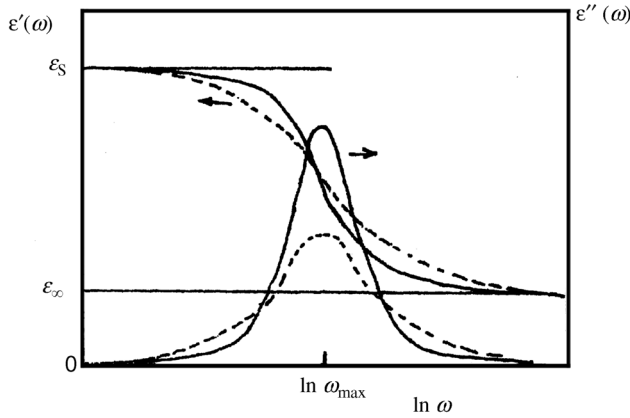


Figure 1.1 General frequency dependence of ε' and ε'' . —, Debye dielectric; ---, real dielectric. Adapted with permission from Ref. [3]; © 1996, Pergamon/Elsevier.

impedance $Z(\omega)$. The latter is related to $\varepsilon(\omega)$ according to Equation 1.4.

$$\varepsilon(\omega) = \frac{1}{j\omega Z(\omega)C_0} \quad (1.4)$$

From the dielectric function, the relaxation time can be extracted as a fitting parameter based on empirical functions. In the simplest case, the Debye function Equation 1.5 is applicable.

$$\varepsilon(\omega) = \frac{\varepsilon_s - \varepsilon_\infty}{1 + j\omega\tau} + \varepsilon_\infty \quad (1.5)$$

(see Figure 1.1 for the definition of ε_s and ε_∞)

Corresponding relations for ε' and ε'' are given by Equations 1.6 and 1.7, which show that the magnitude of the dielectric loss is governed by the relaxation time τ , more exactly speaking by the term $(\omega\tau)^2$ [3].

$$\varepsilon'(\omega) = \frac{\varepsilon_s - \varepsilon_\infty}{1 + \omega^2\tau^2} + \varepsilon_\infty \quad (1.6)$$

$$\varepsilon''(\omega) = (\varepsilon_s - \varepsilon_\infty) \frac{\omega\tau}{1 + \omega^2\tau^2} \quad (1.7)$$

Alternating orientation polarization is feasible at frequencies ranging from $\nu = 0$ (steady field) to about $\nu = 10^{12}$ Hz (lowest IR frequency). At higher frequencies, the dipoles can no longer follow the variations of an external alternating electric field, and here only electron distortion polarization is possible. In the frequency range from 0 to 10^{12} Hz, ε' decreases monotonically from the highest value $\varepsilon' = \varepsilon_s$ at $\nu = 0$ (static dielectric constant) to the lowest value $\varepsilon' = \varepsilon_\infty$ (dielectric dispersion) at the upper limit of ν . On the other hand, ε'' equals zero at $\nu = 0$ and at far IR frequencies. However, at intermediate frequencies, Equation 1.7 predicts a

symmetrical peak at $\omega\tau = 1$, corresponding to $\varepsilon'' = (\varepsilon_s - \varepsilon_\infty)/2$. The general frequency dependence of ε' and ε'' is demonstrated in Figure 1.1.

In many cases – including amorphous polymers – the peaks in dielectric spectra ($\varepsilon'' = f(\omega)$) are not symmetrical and are broader than predicted by the Debye model (Equation 1.7). To account for asymmetry and broadness of the spectra, modified equations characterized by the addition of exponential parameters to Equation 1.5 have been proposed. For example, the *Havriliak–Negami equation* (Equation 1.8) contains two exponents, α and β [4]:

$$\text{Havriliak-Negami equation} \quad \varepsilon = \frac{\varepsilon_s - \varepsilon_\infty}{(1 + (j\omega\tau)^\alpha)^\beta} + \varepsilon_\infty \quad (1.8)$$

In a special case, the symmetry parameter β equals unity. This leads to the so-called *Cole–Cole equation* (Equation 1.9) [5]:

$$\text{Cole-Cole equation} \quad \varepsilon = \frac{\varepsilon_s - \varepsilon_\infty}{1 + (j\omega\tau)^\alpha} + \varepsilon_\infty \quad (1.9)$$

As can be seen from Figure 1.2, the typical dielectric response of a polar amorphous polymer at constant temperature is characterized by a succession of descending steps in ε' and a corresponding series of ε'' peaks.

The multiplicity of dielectric relaxations becoming obvious from this graph reflects various different modes of orientation polarization occurring at distant frequencies. The α -relaxation at the lowest frequencies corresponding to the longest relaxation times is associated with the glass transition – that is, movements of the main chains of the polymer via cooperative motions of main chain segments. The subsidiary β - and γ -relaxations at higher frequencies corresponding to shorter relaxation times are related to motions of single structural elements including rotations and/or conformational changes of side groups.

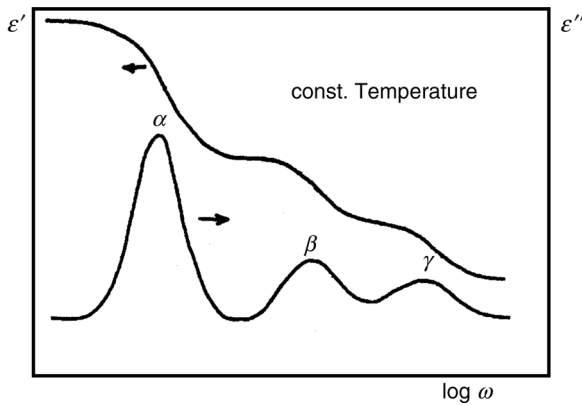


Figure 1.2 Typical dielectric response of a polar amorphous polymer. Frequency dependence of ε' and ε'' at constant temperature. Adapted with permission from Ref. [3]; © 1996, Pergamon/Elsevier.

As sub-THz radiation penetrates a *lossy* dielectric ($\epsilon'' > 0$), energy is dissipated and, therefore, the power of the radiation is attenuated. Equations relating the absorbed dose rate and the penetration depth with ϵ' and ϵ'' can be derived from Maxwell's equations; details (not given here) for this are available from the relevant literature [3,6].

The absorbed dose rate – that is, the radiation energy absorbed per volume and time unit – is given by Equation 1.10 [6]:

$$D_r^{\text{abs}} = 2\pi\nu\epsilon_0\epsilon'' E^2 \quad (\text{Js}^{-1} \text{ m}^{-3}) \quad (1.10)$$

where ν is the frequency (in Hz) and E is the electric field strength (in V m^{-1}).

The penetration depth, d_p – that is, the depth at which the incident radiation power is being reduced to $1/e$ (about 37%) – is given by Equation 1.11 [6]:

$$d_p = \frac{\lambda_0}{2\pi(2\epsilon')^{0.5}} \left[\left(1 + (\epsilon''/\epsilon')^2 \right)^{0.5} - 1 \right]^{-0.5} \quad (\text{m}) \quad (1.11)$$

For low-loss dielectrics – that is, for $(\epsilon''/\epsilon') \ll 1$, d_p approximates to:

$$d_p = \frac{\lambda_0(\epsilon')^{0.5}}{2\pi\epsilon''} \quad (\text{m}) \quad (1.12)$$

where λ_0 (m) denotes the wavelength *in vacuo*. Obviously, the penetration depth increases with larger wavelengths, that is, with decreasing frequency. This can be seen also from Table 1.3, where d_p values calculated with the aid of Equation 1.12 are listed for various frequencies and ϵ'' values. Typically, at $\nu = 10^9$ Hz, corresponding to $\lambda_0 = 0.3$ m, the penetration depth into poly(ethylene terephthalate), amounts to $d_p = 9.26$ m, with $\epsilon' = 2.4$ and $\epsilon'' = 8 \times 10^{-3}$.

1.1.2.2 Temperature Dependence

The variation of ϵ' and ϵ'' with temperature can be explained on the basis of the Debye model, according to which the absorption of sub-THz radiation in nonionic materials is caused by the orientation polarization of polar molecules or polar groups in polymers and, therefore, depends on the mobility of the polar entities. Since the extent to which absorption occurs via this mechanism is essentially

Table 1.3 Penetration depth d_p (m) of sub-THz radiation into a nonmagnetic material of relative dielectric constant $\epsilon' = 3.0$, and different electric loss factors ϵ'' at various frequencies. Calculated with the aid of Equation 1.12.

ϵ''	Frequency (Hz)			
	10^4	10^6	10^8	10^{10}
0.01	8.27×10^5	8.27×10^3	8.27×10^1	8.27×10^{-1}
0.1	8.27×10^4	8.27×10^2	8.27	8.27×10^{-2}
1.0	8.27×10^3	8.27×10^1	8.27×10^{-1}	8.27×10^{-3}

determined by the relaxation time τ (see Equations 1.6 and 1.7), the temperature dependence of ϵ' and ϵ'' is related to that of τ , as given by Equation 1.13.

$$\tau = \frac{h}{kT} \exp\left(\frac{\Delta G^*}{RT}\right) = \frac{h}{kT} \exp\left(-\frac{\Delta S^*}{R}\right) \exp\left(\frac{\Delta H^*}{RT}\right) \quad (1.13)$$

where h is Planck's constant, k is Boltzmann's constant, and ΔG^* , ΔS^* and ΔH^* denote molar free energy, molar entropy and molar enthalpy of activation, respectively. For a limited temperature range, the pre-exponential and the entropy term can be combined in a practically temperature-independent term τ_0 , as expressed by Equation 1.14:

$$\tau = \tau_0 \exp\left(\frac{\Delta H^*}{RT}\right) \quad (1.14)$$

According to Equation 1.14, $\ln(\tau)$ decreases with increasing temperature, which implies that in plots of ϵ'' versus $\omega = 2\pi\nu$, the peak of the absorption band is shifted to higher frequencies with rising temperature. This results from the fact that, at the peak's maximum, $\omega_{\max}\tau = 1$. Consequently, an increase in temperature resulting in a decrease in τ enforces an increase in ω_{\max} and vice versa, an increase in τ , caused by decreasing temperature, yields a lower ω_{\max} . According to Equations 1.6 and 1.7, the magnitude of ϵ' is determined both by ϵ_∞ and the difference $\epsilon_S - \epsilon_\infty$, and that of ϵ'' by $\epsilon_S - \epsilon_\infty$. These terms depend in different modes on temperature for polymers with polar side groups and polymers containing in-chain or rigidly attached polar groups.

For many compounds, including certain polymers, both ϵ' and ϵ'' increase with increasing temperature. While this increase is marginal with respect to ϵ' , it is quite significant in the case of ϵ'' . Typically, in the case of polyamide 6,6, ϵ'' increases by a factor of about 10 as the temperature rises from 40 to 150 °C (see Figure 1.3).

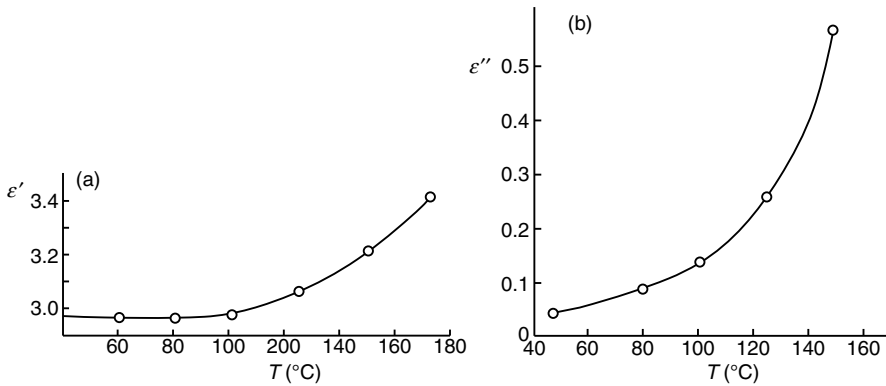


Figure 1.3 Dielectric properties of polyamide 6,6 at 3 GHz. ϵ' and ϵ'' as a function of temperature. Adapted with permission from Ref. [8]; © 1976, International Microwave Power Institute.

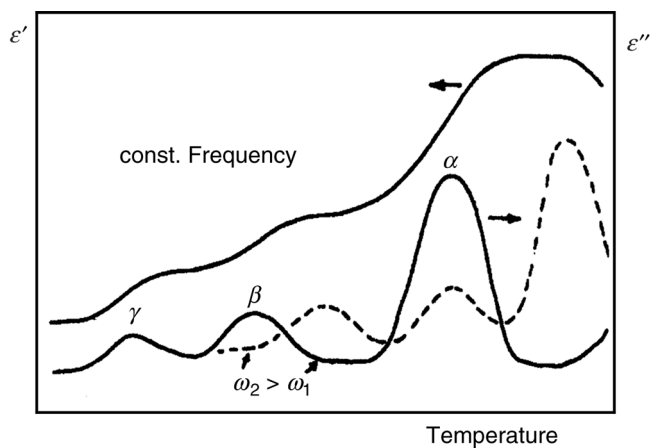


Figure 1.4 Typical dielectric response of a polar amorphous polymer. Temperature dependence of ϵ' and ϵ'' at constant frequency. Adapted with permission from Ref. [3]; © 1996, Pergamon/Elsevier.

It is interesting to note that, in the case of amorphous polar polymers, the temperature dependence of ϵ' and ϵ'' reflects alterations in the physical state of the system. This is due to the fact mentioned above that the absorption of sub-THz radiation is based on the orientation polarization of polar groups, which is determined by their mobility. As a polymeric system is heated up from low to high temperatures, various physical stages related to the mobility of structural elements are surpassed. As demonstrated in Figure 1.4, the temperature dependence of the dielectric response at constant frequency, typical for a polar amorphous polymer, is characterized by a succession of ascending steps in ϵ' and a corresponding series of ϵ'' peaks.

The peak at the highest temperature is associated with the α -relaxation – that is, to the motions of main-chain-segments becoming activated during the glass transition. The subsidiary weaker peaks refer to the β - and γ -relaxations associated with various motions, such as rotation or conformational changes of polar side groups.

It should be noted that a positive $d\epsilon''/dT$ implies an increase in the absorbed dose rate during irradiation, as the latter heats the system up. Therefore, care must be taken during RF- and microwave-aided processing to avoid unwanted overheating, the so-called *runaway effects*.

1.2

Applications in Polymer Chemistry

1.2.1

General Aspects

Materials absorbing sub-THz radiation ($\nu < 10^{12}$ Hz) are rapidly heated up, which is an attractive feature for chemists since, in comparison with conventional heating

techniques, many thermally induced chemical processes can be performed with a substantially shortened reaction time. In fact, reductions from many hours or days to several minutes, or even seconds, are common place.

As was noted in Section 1.1, the absorption of sub-THz radiation by organic materials is restricted to those containing ionic and/or polar components and, in the case of linear polymers, with polar groups incorporated in the main chain or in side chains. Provided that the penetration depth of the radiation is substantially larger than the sample's thickness, heating proceeds *volumetrically* – that is, simultaneously in the total irradiated volume – and does not rely on convection or the conduction of energy from the system's outside to its interior, as in the case of classical heating (such as a hot plate or oil-bath heating). Thus, microwave irradiation represents an attractive and safe alternative to classical heating, as it permits a required reaction temperature to be attained at a much faster rate.

In fact, the mode of action of sub-THz radiation-induced chemical reactions is still under debate [9]. Because of the low photon energy (0.0016 eV at 2.45 GHz), sub-THz radiation cannot break chemical bonds (which have binding energies of several eV), and so such radiation cannot directly induce chemical reactions. Therefore, frequently observed microwave effects – such as an acceleration of the reaction rate, increases in product yield and variations in product distribution – are commonly interpreted on the basis of purely thermal effects. The latter include very rapid heating, superheating to temperatures that substantially exceed the boiling point of the solvent, or a pressure increase if a closed system is irradiated. The selective excitation of dipoles, causing a large temperature increase in their vicinity and enhanced diffusion rates of small molecules, is thought to be responsible for an increase in reaction rate and a decrease in the apparent activation energy (for details, see Ref. [10]). Moreover, microwave phenomena are explained in terms of changes in thermodynamic properties under the influence of microwave fields [11]. This model comes close to speculations on *nonthermal radiation effects* that are still lacking convincing evidence [9]. On the other hand, nonthermal reactions can be induced by *plasmas* generated by sub-THz radiation, and plasma-assisted chemistry is widely applied in industrial processes, for example in processes related to the field of polymers.

Apart from the role that sub-THz radiations play in polymer chemistry, they are also very usefully applied in polymer physics. As an example, this might involve dielectric spectroscopy, which is used widely to characterize the molecular dynamics of polymers. Moreover, microwaves are employed for the nondestructive testing of polymer materials, an example being the detection of heterogeneities in plastic articles.

1.2.2

Thermal Effects

The advent of commercial laboratory microwave reactors and the corresponding industrial-scale equipment [10] has given rise to worldwide activity concerning the

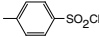
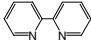
sub-THz radiation-assisted synthesis of organic compounds. Indeed, a plethora of reports has been made on the influence of microwave heating on chemical reactions with organic compounds [10,12–15]. Although most of these reports have involved the organic chemistry of low-molar-mass compounds, a respectful fraction is related to the field of polymers, including their synthesis via the polymerization of small molecules, the modification and degradation of polymers, and the use of polymer supports for solid-phase organic syntheses [9,16–20]. These topics are discussed in the following subsections.

1.2.2.1 Polymer Synthesis

Chain-Growth Polymerizations

Free-Radical Polymerization The free-radical polymerization of unsaturated compounds is readily performed with the aid of microwaves, provided that the monomer molecules have a permanent dipole moment and can, therefore, absorb microwaves. The classical polymerization mechanism – as described in textbooks [21–24] and involving steps of initiation, propagation, and termination – applies to the microwave-assisted polymerization. Prescriptions for milliliter-scale polymerizations have been described by Bogdal [18], and some typical cases are listed in Table 1.4. Whereas styrene (an unpolar monomer) polymerizes only very slowly if irradiated in bulk, the aqueous emulsion polymerization of styrene using potassium persulfate as an initiator proceeds very rapidly. This process is shown in Figure 1.5, where the conventional and microwave-initiated polymerizations are compared by plotting monomer conversion versus reaction time [25].

Table 1.4 Microwave-assisted free-radical polymerizations of unsaturated monomers at 300 W [18].

Monomer	Polymer	Initiator	Solvent ^{a)}	Reaction time and temperature	Polymer yield (%)
Methyl methacrylate	Poly(methyl methacrylate)	AIBN ^{b)}	Toluene	10 min 90 °C	>50
Isooctyl acrylate	Poly(isooctyl acrylate)	AIBN ^{b)}	Hexane	10 min 65 °C	>60
9-Vinylcarbazole	Poly(9-vinylcarbazole)	AIBN ^{b)}	Toluene	10 min 65 °C	>75
Styrene	Polystyrene	 Cu Br		120 min 110 °C	>50
					

a) Monomer concentration: (ca. 50%, v/v).

b) 2,2'-Azobis(2-methylpropionitrile).

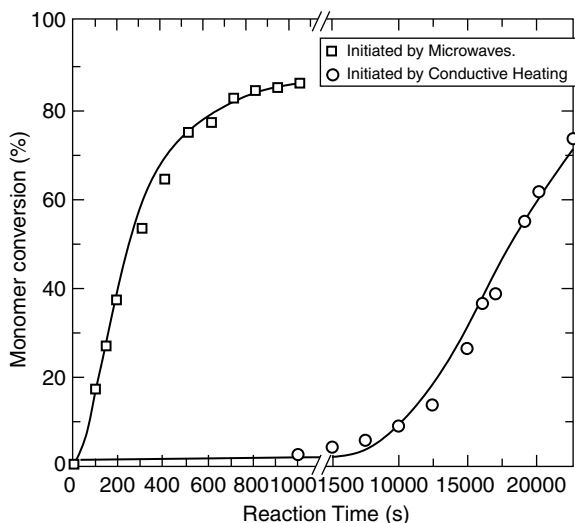
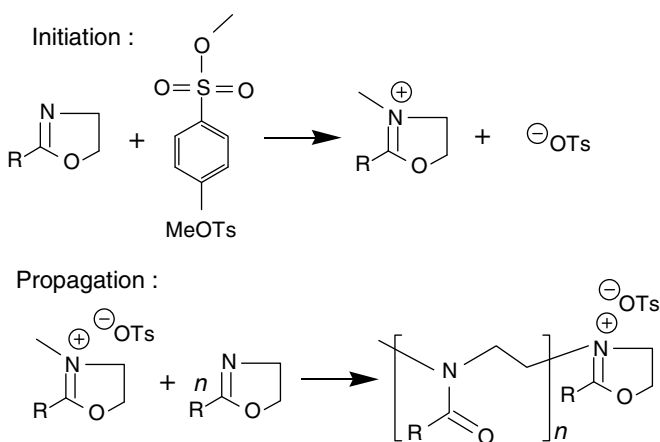
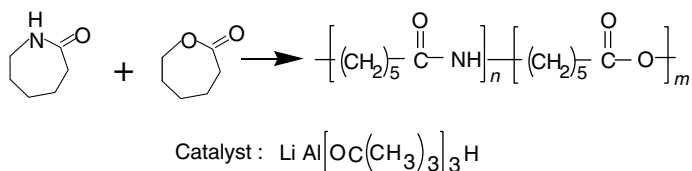


Figure 1.5 Conventional and microwave initiated emulsion polymerization of styrene. Adapted with permission from Ref. [25]; © 1996, VNU Science Press.

Ionic Polymerization A variety of polymerizations that proceed by ionic mechanisms are promoted if microwave heating is applied. Typical cases pertain to the living cationic ring-opening polymerization of 2-oxazolines [10,26] (see Scheme 1.1) and the anionic homo- and copolymerization of ϵ -caprolactone and ϵ -caprolactam [27] (see Scheme 1.2). The rate of polymerization of 2-ethyl-2-oxazoline at 200 °C in acetonitrile solution is accelerated by a factor of 400 as compared to conventional heating [26]. Notably, poly(2-ethyl-2-oxazoline), being both biocompatible and biodegradable, is applicable to drug-delivery systems.



Scheme 1.1 Ring-opening polymerization of 2-oxazolines. R: methyl, ethyl, nonyl, or phenyl [26].



Scheme 1.2 Copolymerization of ϵ -caprolactam and ϵ -caprolactone [27].

ϵ -Caprolactone and ϵ -caprolactam, both of which are polar compounds capable of absorbing microwaves, were shown to homopolymerize more rapidly in catalyzed, solvent-free processes under microwave heating (at 4.2 to 5.2 GHz) than with conventional heating, producing yields of 92% and 87%, respectively [27]. The molar mass, melt temperatures and glass transition temperature (T_g) of the homopolymers obtained by the two heating methods were of comparable magnitude. The microwave-assisted anionic copolymerization of the two compounds, catalyzed by lithium tris-*tert*-butoxyalumino hydride, resulted in polymers with a molar mass of approximately $2 \times 10^4 \text{ g mol}^{-1}$ (yield: ca. 70%). The yields, amide-to-ester ratios and T_g -values were higher, and the molar masses of products equivalent, as compared to those obtained by conventional heating.

Subsequent studies on polymerization of the bisaliphatic epoxy compound 3,4-epoxycyclohexylmethyl, 3,4-epoxy-cyclohexylcarboxylate (see Chart 1.1) revealed that the compound does not polymerize thermally in the absence of an initiator. However, in the presence of diaryliodonium or triphenylsulfonium salts, an ionic polymerization was initiated and the onset of the polymerization shifted to higher temperatures upon microwave heating (see Table 1.5). This microwave effect could be explained in terms of the thermodynamic properties being different under the influence of a microwave field [11].

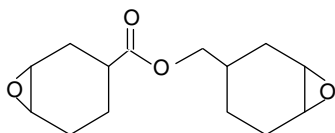
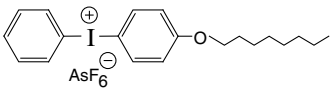
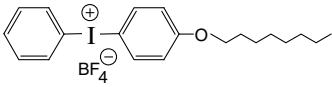
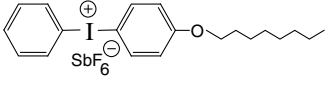


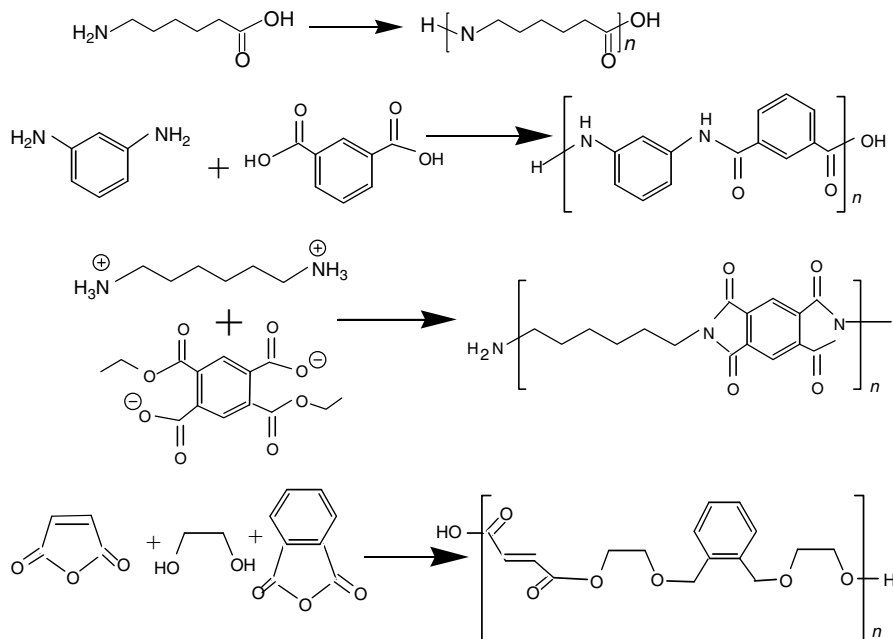
Chart 1.1 Chemical structure of 3,4-epoxycyclohexylmethyl,3,4-epoxy-cyclohexylcarboxylate.

Step-Growth Polymerization Microwave-assisted step-growth polymerizations – that is, polycondensation and polyaddition reactions – have been studied extensively. According to a review by Wiesbrock *et al.* [10], a plethora of reports has been devoted to the microwave-assisted synthesis of polyamides, polyimides, polyethers, and polyesters. For the majority of polymerizations, the reaction rates were significantly increased under microwave irradiation as compared to conventional heating, whilst in many cases the reaction times were shortened from hours, and sometimes days, to about 10 minutes. Moreover, the product purity was improved and the polymers exhibited superior properties, most likely due to a reduction in

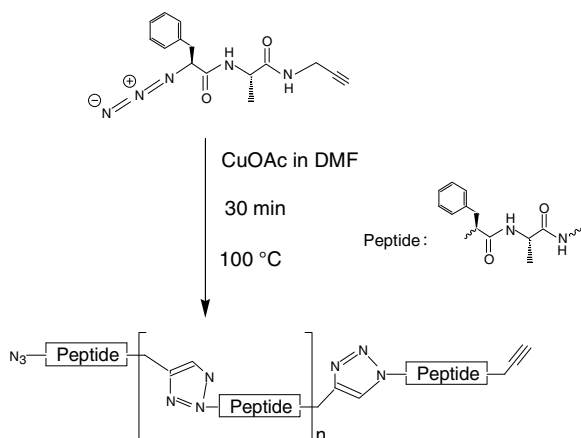
Table 1.5 Polymerization of the epoxide compound shown in Chart 1.1 with the aid of different onium salts. Comparison of the onset temperatures for conventional and microwave heating [28].

Initiator	Conventional heating	Microwave heating
	212 °C	257 °C
	169 °C	216 °C
	191 °C	217 °C

side reactions. A small selection of microwave-assisted step-growth polymerizations, as described in various reports, are presented in Scheme 1.3. It should be noted that these polymerizations were quite often performed in polar solvents with high boiling points, because of the low microwave absorbance of monomers; such solvents included *o*-cresol, dimethylacetamide, and *N*-methylpyrrolidone.

**Scheme 1.3** Microwave-assisted step-growth polymerization. Typical systems [10,18].

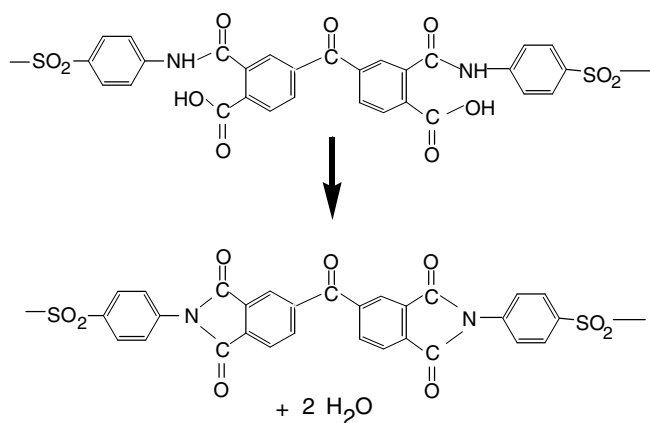
Another interesting example was the synthesis of peptide-based polymers via the Cu(I)-catalyzed N–C polymerization of azido-phenylalanyl-alanyl-propargyl amide [29] (see Scheme 1.4).



Scheme 1.4 Synthesis of peptide-based polymers via Cu(I)-catalyzed N–C polymerization of azido-phenylalanyl-alanyl-propargyl amide in dimethylformamide solution ($c > 250 \text{ g l}^{-1}$). $n = 80$ to 150 [29].

1.2.2.2 Polymer Processing

Thermoset systems including epoxide systems, polyesters, polyimides, and polyurethanes are cured more quickly by microwave heating than by conventional thermal heating. This benefit of microwave heating was concluded from many studies reviewed by Zong *et al.* [19], with one typical example pertaining to the unimolecular imidization of a polyamic acid in *N*-methylpyrrolidone solution (see Scheme 1.5).

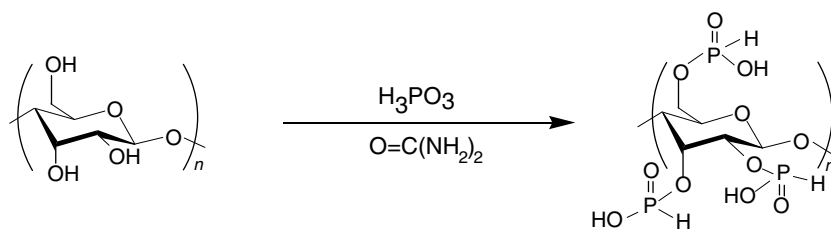


Scheme 1.5 Imidization of a polyamic acid [30].

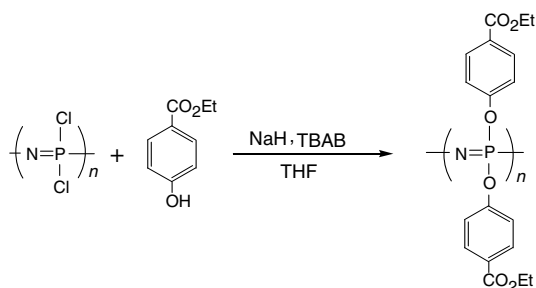
According to Lewis *et al.* [30], the rate constant of the imidization is increased and the activation energy reduced when the reaction is performed with microwaves rather than with conventional heating. In contrast to most other studies, however, Mijovic *et al.* found no difference in curing rates upon investigating epoxide systems and polyimides [31].

1.2.2.3 Modification of Polymers

There is a significant potential of microwave-assisted modification of linear polymers via side group substitution, and the details of two examples pertaining to cellulose and polyphosphazene are presented here. The phosphorylation of cellulose at OH groups, as achieved by the microwave irradiation of a mixture of cellulose, urea and phosphorous acid at 105 °C for 2 h, is shown in Scheme 1.6 [18], while Scheme 1.7 indicates how chlorine atoms of poly(dichlorophosphazene) can be substituted by microwave heating of the polymer in the presence of ethyl-4-hydroxybenzoate, tetrabutyl ammonium bromide (TBAB), tetrahydrofuran (THF), and NaH for 2 h at 65 °C [18].



Scheme 1.6 Modification of cellulose [18].



Scheme 1.7 Modification of poly(dichlorophosphazene) [18].

1.2.2.4 Polymer Degradation

Microwave heating is an appropriate tool for recycling polymer waste. For example, it can be applied to separate metal from polymer/metal laminates by pyrolysis, to depolymerize polyamide and poly(ethylene terephthalate) by solvolysis, or to devulcanize rubber (see Table 1.6). Detailed information on this topic is available in Ref. [19].

Table 1.6 Typical processes based on microwave-assisted polymer degradation.

Process	System	Remarks	Reference
Pyrolysis	HDPE ^{a)} /aluminum laminates	Clean Al is obtained	[32]
	Polysiloxane		
Depolymerization	Polysilazene	Conversion to ceramics	[33]
	Polyamide-6	Solvolytic within 4 to	[34]
	Poly(ethylene terephthalate)	10 min	[35]
Devulcanization	Vulcanized rubber	Cleavage of S–S bond, polymer chain remains intact	[36]

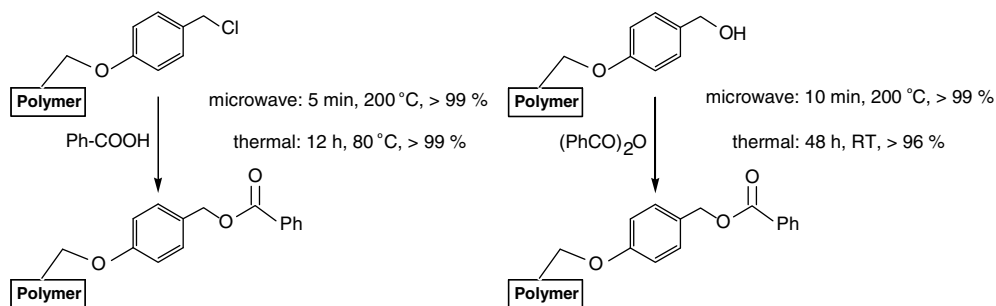
a) HDPE: high-density polyethylene.

One very useful application of the microwave heating technique is in the hydrolysis of proteins and peptides for amino acid analysis [37]. Conventionally, protein analysis is performed by hydrolyzing samples in aqueous 6 N HCl solution at 110 °C for periods of at least 24 h, in conjunction with high-performance liquid chromatography (HPLC). By employing microwave heating, however, the reaction time can be reduced to less than 1 h, and in special cases to a few minutes. As microwave hydrolysis accelerates the reaction without altering the chemistry of amino acid analysis, the same acids, protective agents and derivatization procedures can be used as are employed in conventional processes. Interestingly, microwave heating is also appropriate for the generation of HCl vapor in the vapor-phase hydrolysis of proteins [37].

1.2.2.5 Polymer Supports for Solid-Phase Organic Synthesis (SPOS)

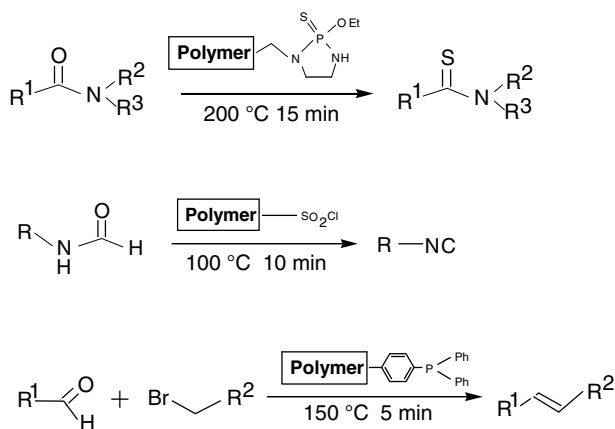
Based on the Merrifield synthesis for the preparation of peptides, SPOS using insoluble polymer supports has been developed for the rapid preparation of large libraries of small organic molecules with drug-like properties. Notably, SPOS contributes essentially to the field of *combinatorial chemistry*, which is the art and science of synthesizing and testing compounds for their bioactivity, aiming at the discovery of new drugs.

The polymer supports employed commonly include crosslinked polystyrene and membranes of polypropylene and cellulose. The general SPOS procedure involves several steps: following attachment of the educt to the polymer support, the latter is contacted with a solution of a reagent and subsequently heated to the desired temperature. This procedure can be repeated using a second or third reagent, after which the product is finally detached from the support and isolated. The main shortcomings of this method – notably the long reaction times required – can be overcome by using microwave heating (mostly with 2.45 GHz radiation), and significant increases in the reaction rates, yields, and purity of products have been observed [14,38,39]. A typical extent of rate enhancement is shown in Scheme 1.8, where the reaction times using conventional thermal and microwave heating are compared [40].



Scheme 1.8 Typical examples demonstrating rate enhancement in the case of microwave-assisted solid-phase organic synthesis [40].

As an alternative approach, instead of performing the process with educts coupled to the support, polymer-supported reagents (PSRs) can be brought into contact with the educt dissolved in an appropriate solvent. In this case, the polymer support can be easily isolated from the product solution by filtration. Moreover, it is possible to apply a surplus of the PSR, and this frequently leads to higher product yields. Microwave heating has also been used to improve the PSR method, and some typical microwave-assisted reactions are shown in Scheme 1.9. More detailed information on this topic, and some appropriate references, are provided in Ref. [14].



Scheme 1.9 Typical examples of microwave-assisted reactions with polymer-supported reagents [14].

Another occasionally useful alternative to the above-described methods is to employ a liquid-phase synthesis on soluble polymeric supports. In this case, the reactive molecules such as poly(ethyleneoxide) are coupled to a polymer backbone and brought into contact with reagents within a homogeneous medium (solvent). On completion of the reaction, the polymeric matrix is separated from the system

by precipitation, membrane filtration, or size-exclusion chromatography. The large number of thiohydantoin of the structure shown in Chart 1.2, and which have been synthesized in this way, represent an example of this approach [41]. Notably, the use of microwave heating led to a significant acceleration in the different steps of the process.

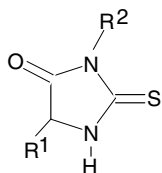


Chart 1.2 General structure of thiohydantoin prepared by microwave-assisted liquid-phase synthesis on poly(ethylene oxide) of molar mass 6000 g mol^{-1} .

It should be noted that solvents employed in microwave-assisted synthesis on polymer supports must fulfill various requirements. In particular, they should swell the polymer, have a high boiling point, exhibit a high chemical stability and last, but not least, they should absorb microwaves (i.e., they should possess a high ϵ'' -value). 1-methyl-2-pyrrolidone (NMP; see Chart 1.3) fulfills these requirements, at least if used in conjunction with polystyrene supports, which swell strongly in this solvent.

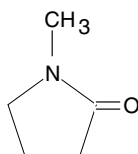


Chart 1.3 Chemical structure of 1-methyl-2-pyrrolidone (NMP).

1.2.3

Non-Thermal Effects

1.2.3.1 Unresolved Questions

Sub-THz radiation – especially microwave radiation – is a powerful tool for initiating classical thermal chemical reactions (as noted in Section 1.2.2). The most obvious sub-THz radiation phenomenon relates to the significantly reduced reaction times, which can be interpreted in terms of the efficient and rapid heating of the reaction mixtures. However, many research groups are currently debating the existence of specific, so-called “non-thermal” modes of action regarding the initiation or modulation of chemical reactions. In particular, it has been asked whether the steric course and the chemoselectivity or stereoselectivity of reactions are altered by the influence of sub-THz radiation, as this would result in new products that would not be formed after classical heating. Various aspects

regarding specific microwave effects have been discussed by many authors [10,11,30,42,43], and in particular by Perreux and Loupy [44]. Accordingly, specific effects can be based on selective energy absorption by dipoles, with ensuing specific reactions of the latter. A temperature increase of 50 K in the vicinity of the absorbing dipoles has been predicted [30], a consequence of which would be an enhancement of the diffusion rates of small molecules. This situation would apply, for example, to the increase in reaction rate and decrease in apparent activation energy in ring-closing imidization reactions [42].

Specific effects are also feasible for reactions proceeding via polar transition states, which can give rise to an enhanced absorption of sub-THz radiation and thus influence the course of the reaction [44]. A typical case refers to the reaction of amines with ketones (see Scheme 1.10).



Scheme 1.10 Amine addition to a carbonyl group involving a polar transition state.

Provided that *thermodynamic properties* such as internal energy and Gibbs free energy of materials with permanent dipole moments undergo significant changes under the influence of microwave fields, shifts in the reaction equilibrium and in kinetics, as compared to thermal fields at the same temperature, can be foreseen [11]. At present, it seems that final conclusions about non-thermal effects can be arrived at only after much more carefully performed experiments have been carried out. However, it is clear that sub-THz radiations – and especially microwaves – can serve as a tool for rapid and efficient heating, with no further influence on most reactions [10].

While the present discussion on non-thermal chemical reactions induced by the direct specific action of sub-THz radiation is ongoing, it is well known that non-thermal reactions can also be initiated indirectly via plasmas generated by the same radiation. In fact, plasma-assisted chemistry is strongly related to the field of polymers, and its importance and major potential for industrial applications are described in the following subsections.

1.2.3.2 Plasma-Assisted Chemistry

General Aspects Radiofrequency or microwave electric fields of sufficient strength can break down a gas under appropriate conditions and produce an electrically conducting medium, denoted as “plasma.” By definition, a plasma is a partially ionized gas, confined to a certain volume with equal numbers of positive and negative charges. The charged particles are free and exhibit a collective behavior. Similar to soap bubbles, plasmas possess at their boundaries a skin called the *plasma sheath* or *Debye sheath*. The main body of a plasma always has a positive

potential relative to the walls, with most of the potential drop appearing across the sheath with voltages ranging from a few volts up to thousands of volts, depending on various parameters. Positive ions generated in the plasma zone are propelled through the sheath and strike the walls or a substrate placed close to the plasma zone at near-normal incidence.

Plasma techniques are employed for the deposition of thin polymer films on solid substrates, for the chemical modification of polymer surfaces, and for the etching of polymer coatings. These processes are usually performed with the aid of low-pressure, low-temperature continuous plasmas, so-called continuous wave (CW) plasmas. Some typical laboratory-scale set-ups for these plasma processes are shown in Figure 1.6 [45].

Plasma etching and plasma film deposition, with the latter frequently being denoted as plasma-enhanced chemical vapor deposition (*PE-CVD*) or somewhat incorrectly as *plasma polymerization*, were initially developed during the 1960s as CW processes. Some years later, processes utilizing afterglow (AG) discharge became very popular, and in many cases these were operated at pressures ranging from 13 to 4000 Pa (0.1 to 30 Torr) and at a field frequency of 13.56 MHz, though

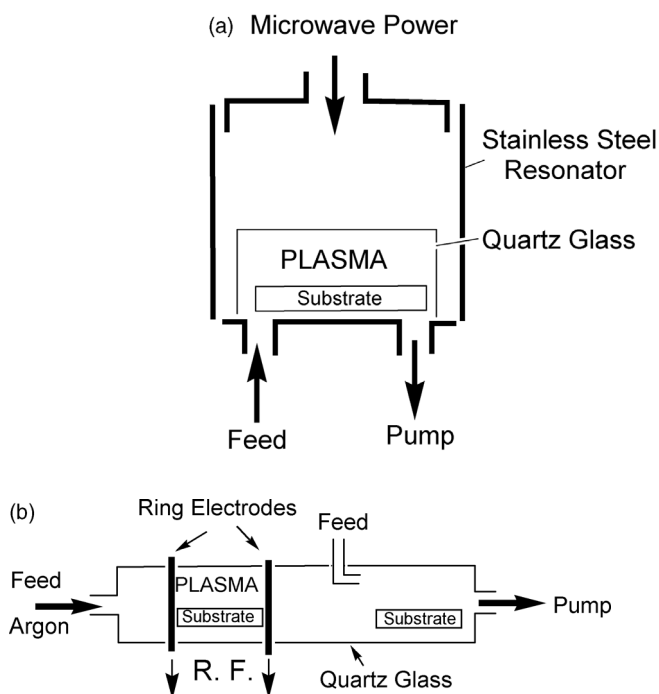


Figure 1.6 Deposition of polymer films with the aid of low-pressure, low-temperature continuous plasmas. (a, b) Typical set-ups with substrates positioned in the plasma zone. The set-up in (b) possesses also a

substrate position downstream from the plasma zone for afterglow deposition. Adapted with permission from Ref. [45]; © 2004, The Electrochemical Society.

frequencies in the kHz and GHz regimes were also utilized. In CW processes, the discharge runs continuously and the substrate is directly exposed to the plasma (in this context, frequently denoted as *glow*). As a result, the substrate is subjected to a direct interaction with reactive neutral and ionized species generated in the plasma by ionization and fragmentation of the feed molecules. In this way, thin films of highly crosslinked, quite irregular macromolecular structures (see Chart 1.4) are formed at the substrate's surface, when the molecular fragments eventually combine.

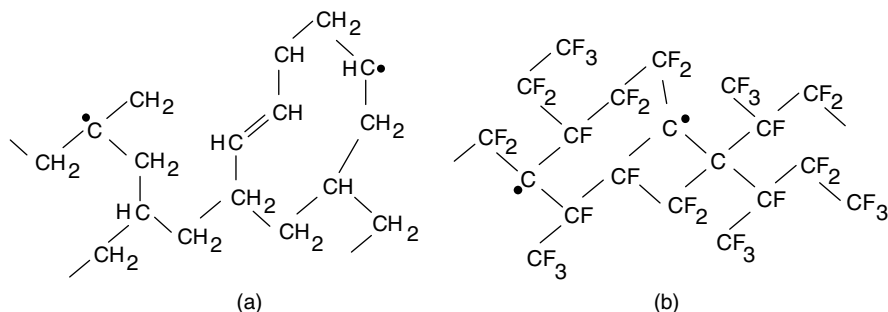


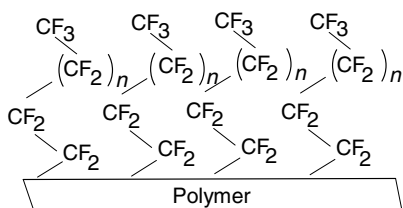
Chart 1.4 Chemical structures of macromolecular coatings formed by deposition at solid substrates positioned in the plasma zone using (a) an aliphatic hydrocarbon feed and (b) a fluorocarbon feed (b).

Commonly, these structures are referred to as *plasma polymers*, although they do not resemble conventional polymers with regular structural repeating units. Practically all organic substances of sufficiently high volatility can be employed for PE-CVD; for example, thin polymer films can form at the surface of appropriate substrates using plasmas generated from aliphatic or aromatic hydrocarbons such as methane, ethane and hexane or benzene and xylene, respectively. Halogenated compounds such as CF_4 and $\text{C}_2\text{F}_3\text{Cl}$, and organosilicon compounds such as tetramethylsilane, hexamethyldisiloxane and hexamethyldisilazane, can also be plasma-polymerized. Conventional monomers suitable for the plasma deposition of polymeric coatings include acrylic acid, allyl alcohol, ethylene, and styrene. A range of compounds that have been used in plasma polymerization studies are listed in Table 1.7. Interestingly, thin polymer films can also be deposited from plasma generated from a gas mixture consisting of CO_2 , H_2 , and NH_3 .

In AG processes, the substrates are positioned downstream with respect to the plasma zone (see Figure 1.6b). Here, the substrate is not bombarded by ions but reacts only with longlived reactive species (especially free radicals) which are following the stream originating from the plasma. More regular macromolecular chemical structures with a high retention of the monomer structure are formed in this way, as indicated in Chart 1.5, which shows the chemical structure of a film deposited from C_2F_6 plasma onto a polymer substrate. Notably, in the case of AG PE-CVD the deposition rate is several orders of magnitude lower than for PE-CVD.

Table 1.7 Selected compounds employed in plasma polymerization studies [46].

Class	Monomer
Hydrocarbons	Methane, ethane, hexane benzene, toluene, xylene, naphthalene, hexamethylbenzene
Halogenated hydrocarbons	Tetrafluoromethane, trifluorochloroethylene
Unsaturated compounds	Ethylene, tetracyanoethylene, propylene, isobutene, acrylic acid, allyl alcohol, allyl amine, vinyl trimethyl silane, acetylene
Organosilicon compounds	Tetraethyloxysilane, hexamethyldisiloxane, tetramethylsilane, hexamethyldisilazane
Sulfur-containing compounds	Thianthrene, thiophene, thioacetamide, thiourea
Nitrogen-containing compounds	Aniline, <i>p</i> -toluidine, picoline
Other compounds	Diphenyl mercury, diphenyl selenide

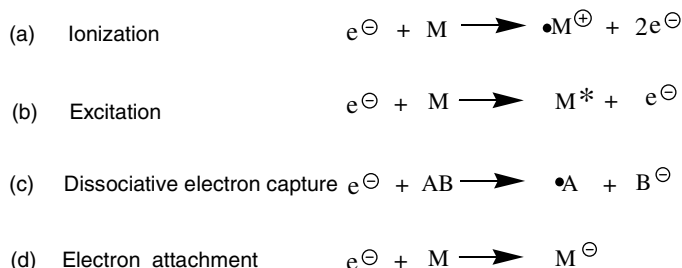
**Chart 1.5** Chemical structure of a film deposited on a polymer substrate from C_2F_6 plasma by afterglow plasma-enhanced chemical vapor deposition (AG PE-CVD) [47].

A high degree of monomer structure retention can be achieved also by employing a modulated plasma technique. In this case, the power input is delivered to the plasma for a period t_{on} and switched off for a period t_{off} , with $t_{off} \gg t_{on}$. As the substrate is positioned in the plasma zone, it is subjected to attack by reactive particles during the on-period, while reactive species that have been generated on its surface react with intact feed molecules during the off-period. Provided that the feed contains a conventionally polymerizable compound, the short plasma pulse will initiate its polymerization, exactly speaking the graft-copolymerization of the monomer at the polymer surface.

The great interest in the field of plasma-assisted chemistry is reflected by a large number of reviews and books [45,46,48–62], and by two journals devoted to the subject [63,64].

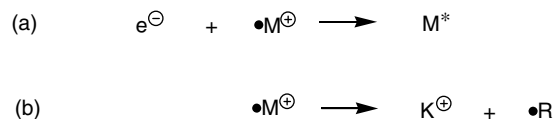
Mechanistic Aspects Usually, the breakdown of gases under the influence of an alternating electric field is initiated by a relatively small number of electrons produced from an external agency. These electrons acquire kinetic energy mainly from the electric field, and partially from elastic collisions with gas molecules. Upon multiplication of these processes, the kinetic energy of the electrons

eventually becomes sufficiently high to accomplish electronic excitations and ionizations of feed molecules by electron impact (see reactions (a) and (b) in Scheme 1.11). The ionization produces additional electrons. It should be noted that the kinetic energy of the primary electrons is reduced by these processes. Subsequent fragmentation processes yield a variety of intermediates that include radical cations and free radicals. Negative ions can be formed by attachment processes of *sub-excitation electrons with gas molecules* (see reactions (c) and (d) in Scheme 1.11) [65]. Sub-excitation electrons have kinetic energies below the first electronic excitation potential of the feed molecules.



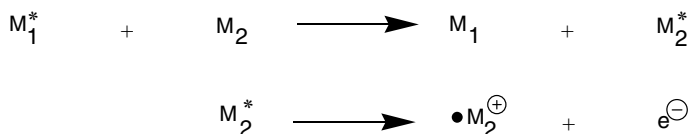
Scheme 1.11 Reactions of electrons with plasma feed molecules. The asterisk denotes an electronically excited state.

After having lost their kinetic energy, the electrons combine with positive ions, typically according to reaction (a) in Scheme 1.12. Often, radical cations disintegrate spontaneously into smaller cations and free radicals according to reaction (b) in Scheme 1.12.



Scheme 1.12 Reactions of radical cations. The asterisk denotes an electronically excited state.

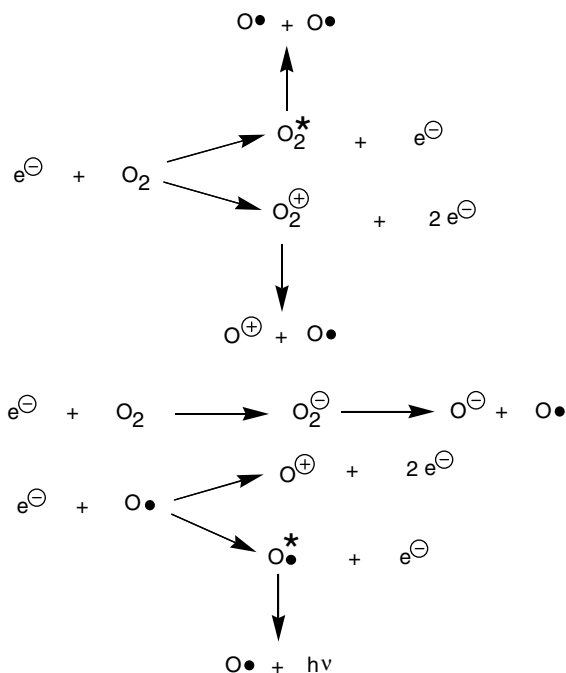
Energy transfer from excited molecules M_1^* to molecules M_2 of a lower ionization potential might also result in ionization; this process is referred to as *Penning ionization* (see Scheme 1.13).



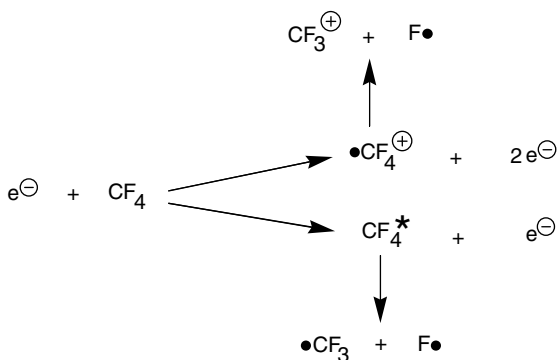
Scheme 1.13 Energy transfer from molecules of high ionization potential to molecules of lower ionization potential, resulting in ionization (Penning ionization). The asterisk denotes an electronically excited state.

Typical reaction schemes related to plasmas applied to the fabrication of microelectronic devices are presented in Schemes 1.14 and 1.15 (the former scheme refers to an oxygen plasma and the latter to a CF_4 plasma).

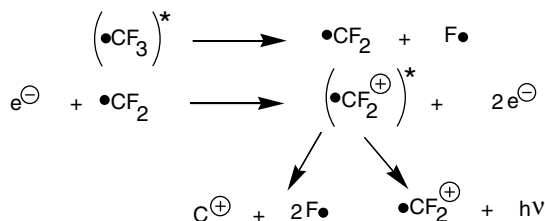
Actually, various fragments including CF_3^\oplus and CF_2^\oplus ions; CF_3 , CF_2 , CF radicals and F atoms have been detected in CF_4 plasmas, indicating the occurrence of additional processes such as those described in Scheme 1.16.



Scheme 1.14 Reactions of electrons in oxygen (O_2) plasmas. The asterisk denotes an electronically excited state.



Scheme 1.15 Reactions of electrons with tetrafluoromethane. The asterisk denotes an electronically excited state.



Scheme 1.16 Processes occurring in a CF_4 plasma [66]. The asterisk denotes an electronically excited state.

A plasma formed by ionization of the feed molecules is maintained if the rates of charge production and charge loss are equal. Charge loss occurs by neutralization – that is, via the combination of electrons or negative ions with positive ions, and reaction (a) in Scheme 1.12 is a typical example of this. Details concerning breakdown mechanisms and the maintenance of fully developed plasmas have been described in detail (e.g., Ref. [6]).

If a substrate is to be plasma-modified, then photochemical processes must also be taken into account. This follows on from the fact that some of the electronically excited molecules emit photons (see Equation 1.15), which makes the plasma visible (via glow discharge).



To some extent, photons possessing energies corresponding to the UV range are likely to be absorbed by the substrate, thus initiating photochemical reactions. Plasma-induced intermolecular crosslinking and main-chain cleavage, as occurs in the case of substrates consisting of linear polymers, are thought to result from such photochemical processes.

In low-pressure (1 Torr = 133 Pa), high-frequency (1 MHz) plasmas (so-called *nonequilibrium plasmas*), which are of practical importance, the heavy particles (ions and intact molecules) are essentially at ambient temperature, while the electrons are *hot* – that is, they possess kinetic energies that are sufficiently high to cause ionizations and electronic excitations, and under these conditions plasma chemistry takes place at near-ambient temperature. However, the plasma temperature increases as the pressure is increased, and atmospheric plasmas can be applied as heat sources for the activation of endothermic chemical reactions. Relevant investigations with RF plasmas have included the pyrolysis of hydrocarbons such as methane and propane, and the decomposition of carbon tetrachloride [48]. With regards to polymers, surface treatment and thin-film deposition at atmospheric pressure can be performed, when He or Ar are used as carrier gases for the feed, and dielectric insulators are inserted between the electrodes in the discharge gap [67]. Detailed information on atmospheric plasmas, in the context of both thin-film deposition and polymer etching, is available elsewhere [67–69].

Technical Applications Important applications in the field of polymers refer to the plasma etching of thin polymer coatings [70–74] and plasma-induced surface modifications of polymer materials, including polymer coatings [45,49–56,59,70,75–77]. *Plasma etching* – which involves the controlled partial removal of the surface of a body by subjecting the latter to an appropriate plasma – is widely applied in industrial processes. The removal of surface matter can be accomplished by *physical sputtering*, which relates to the removal of surface fragments by a physical process in which energetic positive ions transfer large amounts of energy and momentum to the substrate's surface, thus inducing a mechanical ejection of matter. *Chemical etching* is of greater practical importance than physical sputtering, and is based on the total conversion of surface matter into volatile products by reactions with neutral free radicals. In this case, the mass loss is totally evaporative; for example, a polyimide of the structure shown in Chart 1.6 is totally converted to CO, CO₂, N₂ and H₂O, with the aid of an O₂ plasma.

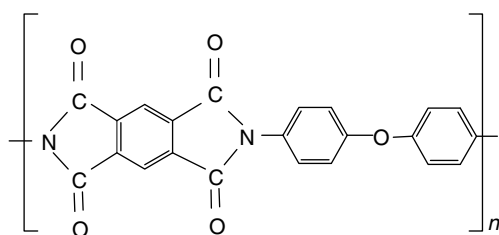


Chart 1.6 Chemical structure of a typical polyimide.

Plasma etching plays a prominent role in the industrial lithographic production of microelectronic devices such as dynamic random access memory (DRAM) chips and micro-electromechanical systems (MEMS), such as accelerometers for airbags in motor vehicles. For these purposes, silicon wafers are generally patterned using sophisticated methods, which results in small structures of dimensions down to the nanometer range. The plasma etching gases presently used in industrial processes are listed in Table 1.8, and the

Table 1.8 Plasma etching gases employed in the production of microelectronic devices [75].

Substrate material	Components of plasma feed
Al	Cl ₂ , BCl ₃ , SiCl ₄ , HBr, HJ
W	HBr, Cl ₂ , O ₂
Si ₃ N ₄	CHF ₃ , CF ₄ , CH ₃ F, SF ₆
SiO ₂	CHF ₃ , CF ₄ , C ₂ F ₆ , C ₄ F ₈
Si	HBr, HCl, Cl ₂ , NF ₃ , CF ₄ , SF ₆ , BCl ₃
Amorphous carbon hardmask	O ₂ , N ₂ /O ₂
Photoresists	O ₂ , N ₂ /O ₂

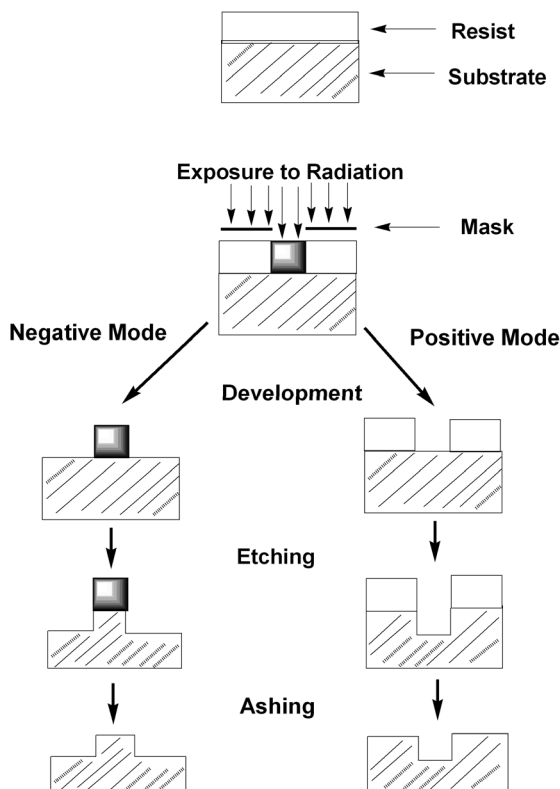


Figure 1.7 Schematic illustration of pattern generation in a silicon wafer employing liquid development: irradiation makes the resist insoluble (negative mode) or soluble (positive mode).

process of pattern delineation is depicted in Figure 1.7. The process starts with a microlithographic step structuring a thin film on top of the wafer; this film, which most often consists of a plasma-resistant polymer (the *polymer resist*) is then subjected to a beam of light, X-rays or swift particles (electrons or ions). The subsequent development of latent structures, generated in this way, with appropriate liquids yields a pattern of covered and uncovered areas on the wafer. After liquid development, trenches and holes at places not covered by the resist are then formed when the wafer is subjected to a specific plasma.

Eventually, the polymer resist – which is not (or only weakly) attacked by the Si- and SiO₂-selective plasmas – is removed totally by a special treatment (referred to as “ashing” or “stripping”) with the aid of an oxygen (O₂) plasma. One outstanding requirement for proper pattern delineation, namely the generation of trenches with vertical walls and flat floors, can be fulfilled by anisotropic (i.e., directional) etching (see Figure 1.8).

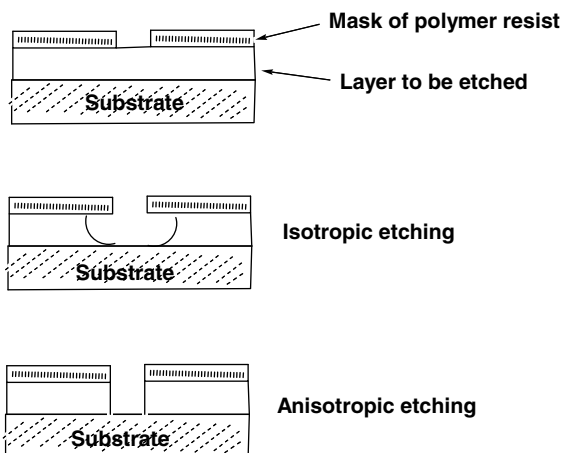


Figure 1.8 Schematic illustration of isotropic and anisotropic etching.

Anisotropic etching is accomplished by ion-enhanced etching, commonly referred to as reactive ion etching (*RIE*). This process is based on the reactions of free radicals with the substrate occurring under the simultaneous bombardment of directed ions. A directional negative-heading electric field that is always formed across the sheath at the plasma boundaries accelerates the positive ions which have been produced in the plasma up to kinetic energies of several hundred eV, and guides them vertically to the wafer's surface. In this way, not only trenches with depths of 10–20 μm (as in the case of DRAM circuits) but also features with depths of 600 μm or more (as afforded in the manufacture of MEMS devices) can be created. The generation of these extraordinarily deep features, which is referred to as *deep reactive ion etching*, may be based on chilling the wafer during etching to 163 K (-110°C), which slows down the chemical reactions of the uncharged, isotropically acting reactive plasma species. Another process alternates repeatedly (up to several hundred times) between two modes. Mode 1 involves an almost anisotropic plasma etch, where ions attack the wafer from a near-vertical direction, while mode 2 involves the plasma deposition of a chemically inert passivation layer. The mode 2 approach protects the entire substrate from chemical attack of uncharged species, while ion etching using mode 1 is restricted to the bottom of the trench.

Surface modifications of polymeric substrates can be performed either with the aid of inorganic gas plasmas (e.g., with oxygen plasmas) or with CVD processes. In both cases the polymer surface is functionalized; that is, any functional groups that profoundly alter the surface properties become chemically attached to the polymer surface. Products obtained with both modification modes are depicted schematically in Figure 1.9.

Generally, the attachment of functional groups to the surface can result in either hydrophilicity or hydrophobicity of the substrate. For instance, it can improve the adhesive strength of polymer surfaces towards differently composed materials.

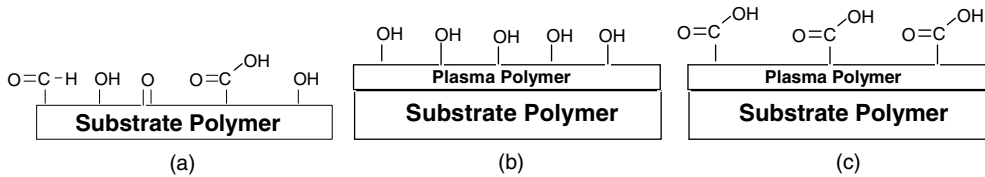


Figure 1.9 Schematic depiction of plasma-induced modifications of polymer surfaces. (a) Unspecific functionalization of the surface of a substrate polymer (e.g., polypropylene) by oxygen plasma treatment; (b, c) Specific functionalization via plasma polymerization of allyl alcohol or acrylic acid, respectively, in the presence of a substrate polymer.

Exactly how the treatment of polymer surfaces with an oxidizing plasma can cause a decrease in the water contact angle (i.e., an increase in wettability) is shown in Table 1.9. Normally, this is related to the surface energy and a reduction in surface energy will indicate a better bondability – that is, the ability of a polymer to bond to other materials.

The plasma treatment of a yarn of polymer fibers used for composite reinforcement provides a typical example of the improvement in adherence [78]. The result is an increase in the strength of the final composite, due to the plasma-induced formation of a very thin interphase layer between the fiber and the composite matrix, causing in turn an improved bonding between the two components (see Figure 1.10).

Substrate hydrophilicity is required for the adhesion of certain biomaterials, such as living tissues. This property has an important role for human body implants, such as orthopedic prostheses. A typical case in which substrate hydrophobicity is required relates to an ophthalmologic scenario, when the surfaces of an intraocular polymer lens should preferably not adhere to proteins in order to avoid the formation of inflammatory cells.

Table 1.9 Alterations in the surface wettability of selected polymers by low-pressure plasma treatment. Adapted from Ref. [78].

Polymer	Initial water contact angle (degrees)	Final water contact angle (degrees)
Polyethylene	87	22
Polypropylene	87	22
Polystyrene	72	15
Polyamide	63	17
Poly(tetrafluoroethylene-co-ethylene)	92	53
Poly(ethyleneterephthalate)	76	17
Polycarbonate	75	33
Poly(phenylene oxide)	75	38
Poly(ether sulfone)	92	9
Silicone	96	53

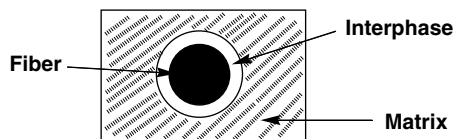


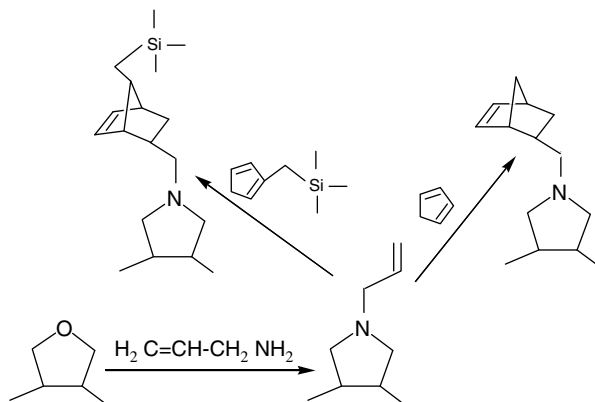
Figure 1.10 Cross-section of a plasma-treated fiber in a composite matrix.

Plasma polymerization leading to functionalized surfaces, as depicted in Figure 1.9b and c, is an outstanding feature of plasma chemistry. Its importance derives from the fact that macromolecular structures can be formed not only from unsaturated substances but also from compounds that are incapable of forming polymers via conventional polymerization techniques. An interesting application here is the plasma-initiated homopolymerization and copolymerization of monomers bearing functional groups on polymer substrates. Relevant investigations have concerned the generation of a very thin adhesion-promoting polymer layer at the surface of polypropylene sheets. By deploying monomers with functional groups (such as allyl alcohol or acrylic acid), plasma polymer layers with up to 30 OH or 25 COOH groups per 100 C atoms can be attached to the surface of the polypropylene substrate, using a pulsed plasma technique with duty cycles of short on-periods and long off-periods, for example, 25 μs to 1200 μs . In this way, good adhesion properties (high peel strength) towards aluminum layers deposited onto the sheet by vacuum evaporation can be attained [53].

Another example relates to the plasma polymerization of maleic anhydride on silicon substrates [55]. After functionalization of the anhydride groups of the polymer with dienophile groups such as allyl amine groups, bicyclo[2.2.1]hept-2-ene groups are attached to the surface via the Diels–Alder cycloaddition of a diene. The cycloaddition of cyclopentadiene or [(trimethylsilyl)methyl]cyclopentadiene to the cyclic imide-functionalized plasma polymer is shown in Scheme 1.17. In this case, the extent to which maleic anhydride groups are converted is controllable, such that the number density of functionalized groups can be tailored to comply with the adhesion between different types of solid surface.

The plasma-assisted surface modification of polymers may also serve to create permselective membranes for gas purification. For example, thin membranes of natural rubber treated with a 4-vinyl pyridine plasma are capable of separating O_2 from N_2 [79]. For additional information on this topic, see Ref. [80].

In conclusion, plasma polymerization provided the possibility to deposit carefully designed, highly adherent and pinhole-free thin polymer films onto various substrates, and thus to control adhesion between various types of solid surface. Moreover, plasma-deposited polymer films can be used to protect metals and other substrates from environmental attacks, for instance by corrosive agents. Further information on these topics is available in Ref. [80].



Scheme 1.17 Attachment of bicyclo[2.2.1]hept-2-ene groups to a cyclic imide functionalized thin layer of plasma-polymerized maleic anhydride [55].

1.3

Applications in Polymer Physics

1.3.1

Dielectric Spectroscopy of Polymers

Dielectric spectroscopy (DS), which is related to measurements of the complex dielectric permittivity $\epsilon^* = \epsilon' - j\epsilon''$, has been used widely to study the dynamics of polymers, including heterogeneous polymer-containing systems [81–87]. DS complements other methods based on nuclear magnetic resonance (NMR), light scattering, and dynamic mechanical analysis. With the aid of commercially available instruments covering a broad frequency range of many orders of magnitude (10^{-6} Hz to 10^{12} Hz), it is possible to investigate molecular motions on quite different time scales, including fluctuations within base units, side group rotations, and cooperative glass transitions. One prerequisite for the application of this technique, however, is the presence of dipoles – that is, in the case of linear polymers of polar groups in the main chain and/or in pendant groups.

With regards to the performance of DS measurements, two modes have been identified: (i) measurements in the frequency domain; and (ii) measurements in the time domain [88–90]. These two terms refer to measurements of ϵ'' as a function of radiation frequency and of time, respectively. Details of, and references pertaining to, the measuring techniques are outlined by Kremer and Schönhal's [88].

A typical example referring to frequency domain measurements is shown in Figure 1.11, where ϵ'' , recorded with poly(methylacrylate) at various temperatures, is plotted as a function of frequency. The two peaks, related to α relaxation (low-frequency) and β relaxation (high-frequency) are shifted to higher frequencies with increasing temperature (details of this phenomenon were outlined in Section 1.1.2.2). It should be noted that the α -relaxation is

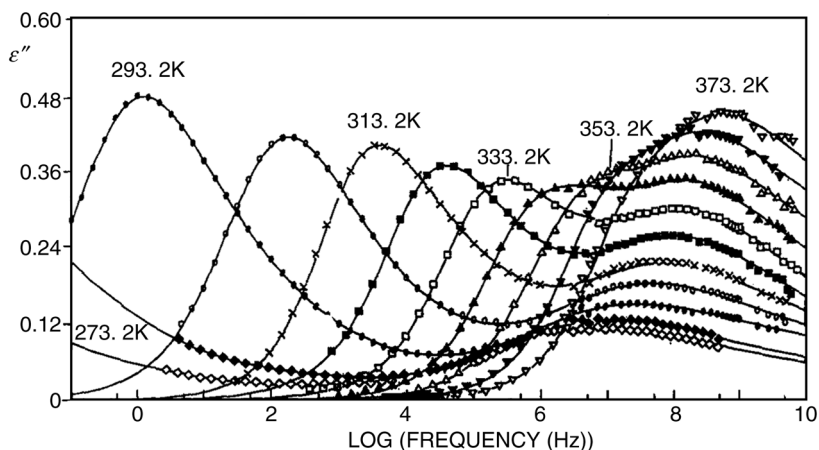


Figure 1.11 Dielectric loss spectra of poly(methyl acrylate) depicting ϵ'' versus frequency at different temperatures. Adapted with permission from Ref. [91]; © 1992, American Chemical Society.

attributed to a structural process, the dynamic glass transition related to segmental motions, while the β -relaxation originates from localized fluctuations of the dipole vector of the side groups, such as the rotation of methyl groups.

With the aid of modern dielectric spectrometers, real-time observations can be carried out. For example, DS can be used to monitor the curing of thermosetting resins, the absorption of water by polymers, or film formation and coalescence in polymer lattices [92].

In the case of nonpolar polymers such as polyolefins, attempts have been made to perform DS by doping the polymer with additives having a large dipole moment (so-called *dielectric probes*) [93]. Here, as a typical example, studies on atactic polypropylene (*aPP*), doped with 4,4'-(*N,N*-dibutylamino)-(*E*)-nitrostilbene (*DBANS*; see Chart 1.7) of dipole moment $\mu = 8$ Debye, is addressed [94]. Plots of ϵ'' versus temperature for both doped and undoped *aPP* are shown in Figure 1.12.

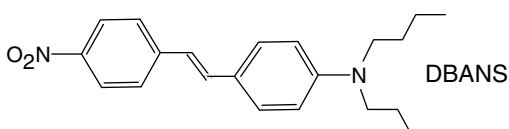


Chart 1.7 Chemical structure of 4,4'-(*N,N*-dibutylamino)-(*E*)-nitrostilbene.

The spectra contained two peaks above and below the T_g (250 K), according to differential scanning calorimetry (*DSC*) at about 150 K and 280 K, which were assigned to the β - and α -processes, respectively. The dopant significantly augmented the α -peak, and in the vicinity of T_g the probe relaxation time τ_α

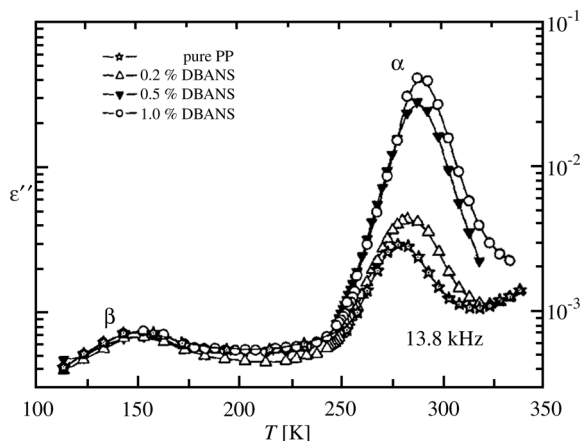


Figure 1.12 Plots of the dielectric loss ε'' versus temperature, recorded at $\nu = 1.38 \times 10^4$ Hz with atactic polypropylene, undoped and doped with different amounts of DBANS. Adapted with permission from Ref. [94]; © 2007, American Chemical Society.

reflected the intrinsic cooperative dynamics of the polymer. The dopant exerted only a very weak plasticizing effect; this was inferred from the fact that, in the presence of the dopant, the T_g values were only slightly lower than T_g (DSC). T_g is obtained, from the temperature dependence of τ_α with the aid of the Vogel–Fulcher–Tamman equation (Equation 1.16).

$$\tau_\alpha = \tau_\infty \exp \left[\frac{E_v}{R(T - T_v)} \right] \quad (1.16)$$

where τ_α and τ_∞ denote the structural relaxation time at temperature T and in the high-temperature limit, respectively, while E_v and T_v are the activation energy and the Vogel temperature, respectively.

More than two decades ago, W. N. Mie *et al.* proposed a model which involved electromagnetic energy coupling through acoustic vibrations along the axis of helical polymers. These authors predicted high absorption cross-sections at microwave frequencies [95], but the prediction could not be verified experimentally [96,97], despite earlier studies seeming to have provided evidence of a resonant microwave absorption of plasmid DNA molecules in aqueous solution in the frequency range 1 to 10 GHz [98]. Such a discrepancy in results is a consequence of pH changes; that is, changes in the ionic conductivity that had not been considered in earlier studies.

1.3.2

Microwave Probing of Electrical Conductivity in Polymers

As noted in Section 1.1, dipole rotation and ionic conduction are the fundamental mechanisms involved when dissipating microwave energy in matter. With regards to

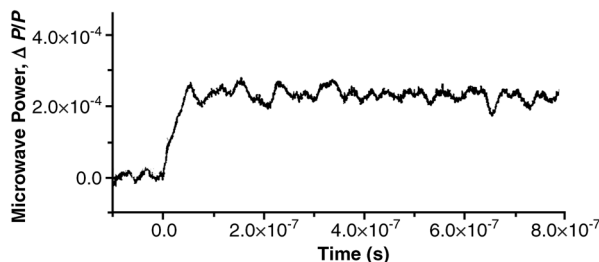


Figure 1.13 Increase in the microwave absorption of poly(methylphenylsilane) at $\nu = 30.4$ GHz, indicating the formation of electrical charge carriers after irradiation with a 12 ns pulse of 266-nm light. Reproduced from Ref. [101].

the ionic conduction mechanism, it is notable that microwave absorption measurements can serve as a very valuable tool for electrode-less electrical conductivity determinations. This may concern, for example, time-resolved measurements, and in this context the method of time-resolved microwave conductivity (TRMC), which is frequently applied to flash photolysis and pulse radiolysis investigations, should be mentioned [99,100]. For example, the TRMC method served to probe charge carriers in polysilanes generated by UV light. The data provided in Figure 1.13 indicate how microwave absorption, expressed here in terms of the relative decrease in incident microwave power, $\Delta P/P_{\text{inc}}$, was increased following the irradiation of poly(methylphenylsilane) with a 12 ns pulse of 266 nm light.

Time-resolved microwave absorption measurements also served to determine the intrachain mobility of charge carriers moving along the chains of ladder-type poly (*p*-phenylenes) and phenylene-vinylene polymers (see Chart 1.8) [102,103]. Upon irradiating O_2 -saturated benzene solutions containing isolated polymer chains (low concentration, 10^{-4} to 10^{-3} base mol l^{-1}) with 10 ns pulses of 3 MeV electrons, benzene cations and excess electrons were generated. Although the electrons were scavenged by oxygen, the cations reacted with the polymer chains via a diffusion-controlled reaction, thus yielding positively charged polymer chains. Eventually, the oxygen anions and polymer cations combined in a neutralization reaction (see Scheme 1.18).

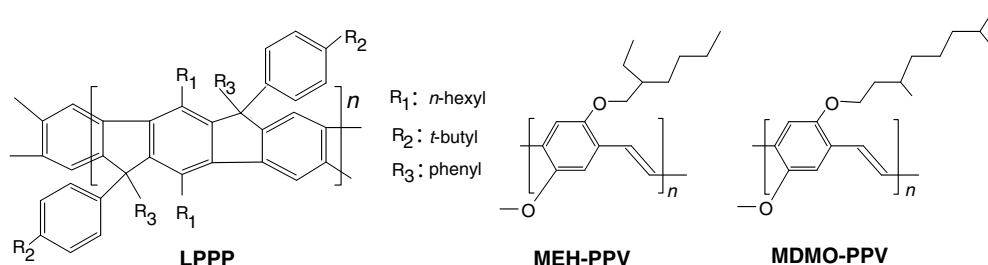
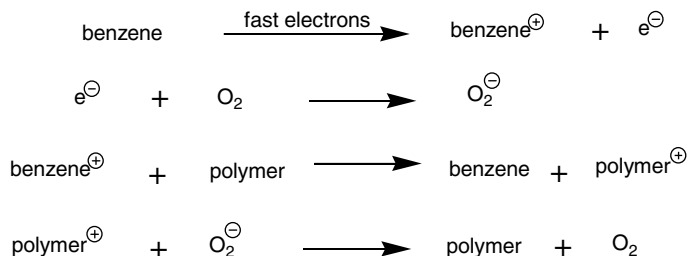


Chart 1.8 Chemical structures of *p*-phenylene and phenylene-vinylene polymers employed for the determination of the intrachain hole mobility [102, 103].



Scheme 1.18 Generation and decay of positively charged polymer chains in O₂-saturated benzene solutions upon irradiation with fast electrons.

The reaction of benzene cations with polymer chains was indicated by an increase in the electrical conductivity of the solution relative to that of neat O₂-saturated benzene (see Figure 1.14). The increase in conductivity was more pronounced the longer the polymer chain length – an effect that was attributed to the fact that the charges diffuse over the entire length of the chains and encounter chain ends within one period of the oscillating electric field. Consequently, the measured intrachain conductivity was seen to be frequency-dependent with a tendency to increase with increasing microwave frequency [104].

The measured electrical conductivity increase of the system $\Delta\sigma(t)$ is related to the mobility of the charge carriers $\mu_{\text{ac},i}$ according to Equation 1.17:

$$\Delta\sigma(t) = e \sum_i \mu_{\text{ac},i} n_i(t) \quad (1.17)$$

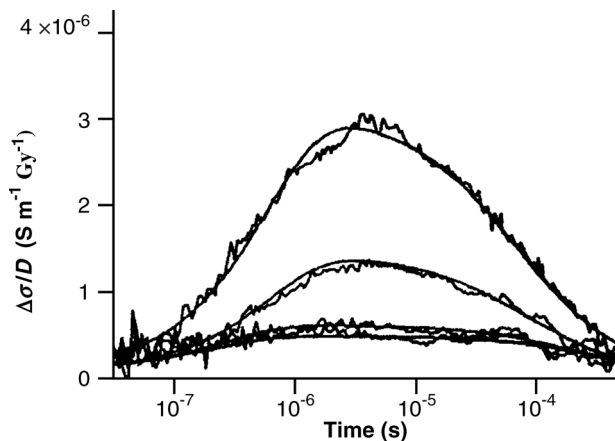


Figure 1.14 Electrical conductivity of benzene solutions containing the ladder-type polymer LPPP (3.15×10^{-4} base mol l⁻¹, average chain length: 13, 16, 35, 54, from bottom to top).

$\nu = 34$ GHz, $E = 20$ V cm⁻¹. Absorbed dose: $D = 21$ Gy. Adapted with permission from Ref. [102]; © 2006, American Physical Society.

where e is the elementary charge and n_i is the concentration of charged species i . Since the mobility of oxygen anions is negligibly small, the sum in Equation 1.17 reduces to the terms related to hole conduction. Moreover, the effective hole mobility μ_{ac} is dominated by the intrachain mobility $\mu_{intra,hole}$, provided that the magnitude of the latter is less than about $0.1 \text{ cm}^2 \text{ V}^{-1} \text{ s}^{-1}$. At higher values of $\mu_{intra,hole}$, scattering of the charge carriers at the chain ends dominated the charge transport and μ_{ac} was much lower than $\mu_{intra,hole}$. On the basis of the chain length dependence of μ_{ac} , and using a theoretical model for one-dimensional diffusive motion of charge carriers between chain ends [104], a very high value of $\mu_{intra,hole}$ (close to $600 \text{ cm}^2 \text{ V}^{-1} \text{ s}^{-1}$) was obtained for ladder-type poly(*p*-phenylene)s (LPPPs) [102]. Therefore, ladder-type polymers such as LPPPs might potentially be used as interconnecting wires in the molecular electronic devices of the future.

Notably, measurements of the electrical conductivity in stretch-oriented polymers such as I_2 -doped polyacetylene, by employing the technique of *coherent microwave transient spectroscopy* [105] revealed a large orientation-dependence. In the case of polyacetylene, the conductivity values parallel and perpendicular to the stretch direction were $\sigma_{||} = 34.4$ and $\sigma_{\perp} = 3.3 \text{ S cm}^{-1}$ [106]. The higher $\sigma_{||}$ -value was believed to be due to the higher electron mobility along the oriented polymer chains. σ -values have been obtained from transmission data with the aid of Equation (1.18):

$$T(\lambda) = \frac{1}{1 + 0.5\sigma L(\mu_0/\epsilon_0)^{0.5}} \quad (1.18)$$

where $T(\lambda)$ is the transmission at wavelength λ , L denotes the sample length, and μ_0 and ϵ_0 are the vacuum permeability and permittivity, respectively [106].

1.3.3

Nondestructive Microwave Testing of Polymer Materials

Microwaves can be applied for the nonintrusive inspection of dielectric materials, including polymers, wood, and ceramics [107–117]. The inspection of dielectric polymeric materials is easily performed, because of their relatively high transparency towards microwaves. Of technical importance are methods based on reflection measurements on sheet materials, such as composites made from several layers adhesively bonded together. In this case, microwave techniques can be used to control composite processing and manufacturing.

Commonly, contact-free measurements with single-sided access to the sample via open-ended rectangular wave guides are performed, as can be seen from Figure 1.15. The signal recorded by the detector results from reflections and interference effects. This serves for the determination of dielectric properties (ϵ' and ϵ''), and of the absolute thickness of thick polymer slabs and dielectric composites made from plastics.

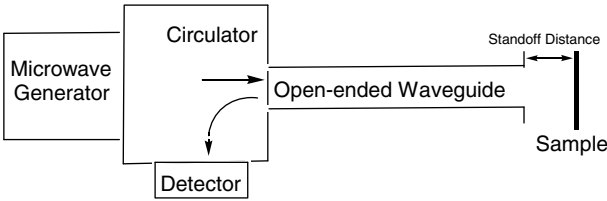


Figure 1.15 Schematic depiction of an open-ended waveguide arrangement for nondestructive inspection of polymer samples.

The importance of microwave nondestructive testing for coatings becomes more obvious when consulting the data in Table 1.10, which elucidate the potential of this method.

With an array of sensors – or, better, with the aid of two-dimensional raster scans – the images of any hidden flaws can be displayed (termed *microwave near-field imaging*). When the sample is located close to the open end of the waveguide, which is commonly referred to as *near-field geometry*, the resolution is about one-tenth of the wavelength. For example, at a frequency of 30 GHz corresponding to $\lambda_0 = 10$ mm, defects at distances of 1 mm can be detected individually. With regards to the determination of thickness variations, a resolution of a few micrometers has been claimed [107].

Thickness measurements on thin polymer layers (25–500 μm) being backed by a metal layer can be accomplished by a method depicted schematically in Figure 1.16. Here, a transmitter/receiver couple is positioned very close to the film surface, where a guided wave is excited. Both the thickness and dielectric properties can be calculated from the signal recorded by the receiver [118,119].

Interestingly, local anisotropies in dielectric materials can be probed and imaged by using a rotating rectangular waveguide which emits linear and polarized microwave radiation. The rotation modifies the relative orientation of the electric field vector, such that dielectric anisotropy will result in a modulation of the measured effective reflection. Both, the modulation depth and the angle of

Table 1.10 Microwave nondestructive testing of dielectric polymeric coatings in noncontact fashion. Access to only one side of the material is needed [107].

Property or Effect	Benefit of the method
Thickness	Determination of absolute values Evaluation of minute variations
Disbonds	Detection of very slight effects
Delaminations	Detection of slight effects
Porosity	Detection of voids and pores, including size estimation
Cracks	Detection of cracks in metals covered with dielectric coatings without the need for removal

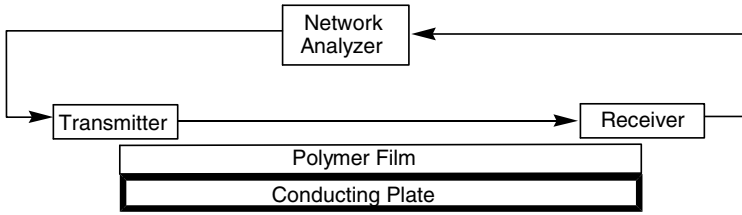


Figure 1.16 Schematic depiction of a set-up allowing nondestructive thickness measurements on thin layers of dielectric polymers. Waves in transverse magnetic

mode launched from the transmitter are reflected from the sample and excite guided modes in the dielectric layer. Adapted from Refs [118,119].

maximum reflection, are related to the extent and the direction of local anisotropies, respectively. In this way, glass fiber-reinforced, injection-molded polymers can be characterized with respect to the orientation of the fibers [113]. As a typical example, the influence of injection speed on fiber orientation is depicted in Figure 1.17 [110].

It is also possible to monitor, during the injection molding of plastic articles, how molds are filled and the melt is cooled down [110]. The curing of resins, determination of the moisture content of polymeric materials, and corrosion phenomena represent further applications of this technique.

Compared to traditional nondestructive testing methods, microwave-based inspection yields a better contrast than X-ray absorption techniques, and a better signal-to-noise ratio than ultrasound inspection. The primary advantages of microwave testing are that measurements can be performed contact-free, and with single-sided access to the sample.

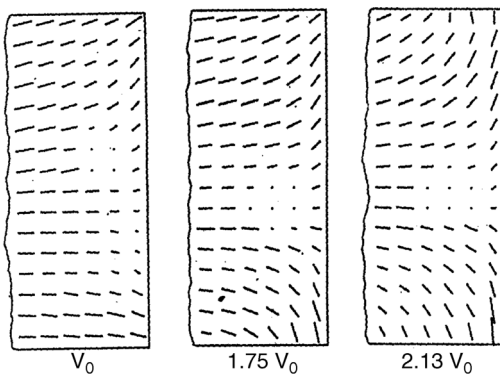


Figure 1.17 Microwave anisotropy images demonstrating the influence of the injection speed (varying between V_0 and $2.13V_0$) on the fiber orientation in the injection molding process. Adapted with permission from Ref. [110]; © 1996, Scientific.Net.

1.4

Industrial Applications

While RF and microwave-based techniques each play important roles in industrial material processing involving plasmas, the use of these radiations as a heating source for thermally initiated chemical reactions is (at present) mainly restricted to the laboratory scale. However, there is one exemption, namely the application of microwave heating to the vulcanization of rubber. Microwave extrusion lines are operated worldwide in the automotive and construction industries for the vulcanization of carbon black-filled rubber [120]. Carbon black is a good microwave absorber, but in the case of white and colored rubbers special sensitizers that permit the absorption of microwaves must first be applied [121].

With regards to plasma applications, both RF- and microwave-based techniques (e.g., low-pressure plasma processes) have been employed since the 1960s for industrial materials processing. At present, plasma techniques are important in those technologies that involve plastics, notably in several areas of the automotive, aerospace, packaging, and textile industries. Although both RF and microwave plasma systems have been developed for specific tasks, plasma processing is generally aimed at increasing the surface energy of films, webs, and fibers so as to achieve better characteristics of printing, bonding wettability and wickability (the ability to transport perspiration away from the human body). Some typical arrangements, as applied to the surface modification of textiles, are shown in Figure 1.18.

It is remarkable, that not only flexible substrates such as films or fabrics but also large stiff objects (e.g., fenders for automobiles) that are made from polypropylene (PP) or ethylene-propylene-diene-terpolymer (EPDM) are plasma-treated on an industrial scale. It should be noted that a large proportion of these applications involve surface modifications for improved adhesion, and that such processes are commonly accomplished with the aid of air or oxygen plasmas [59,123,124].

Finally, the use of plasma techniques for the production of microelectronic devices must be emphasized (see also “Technical Applications” in Section 1.2.3.2), as this involves the technical polymer resist-based generation of microfeatures that now range down to a structure size of 40 nm, allowing a data storage capacity for DRAM chips of up to 2 GByte. Three etching configurations of a parallel-plate plasma reactor applicable to the etching of wafers at low pressure are shown in Figure 1.19. These configurations are distinguished by the manner in which the RF power supply is connected to the electrodes. Plasma etching, in conjunction with the photolithographic structuring of polymer resists, represents a powerful tool that permits a high grade of technical miniaturization that has subsequently led to the creation of products such as personal computers that are today of major importance in daily life.

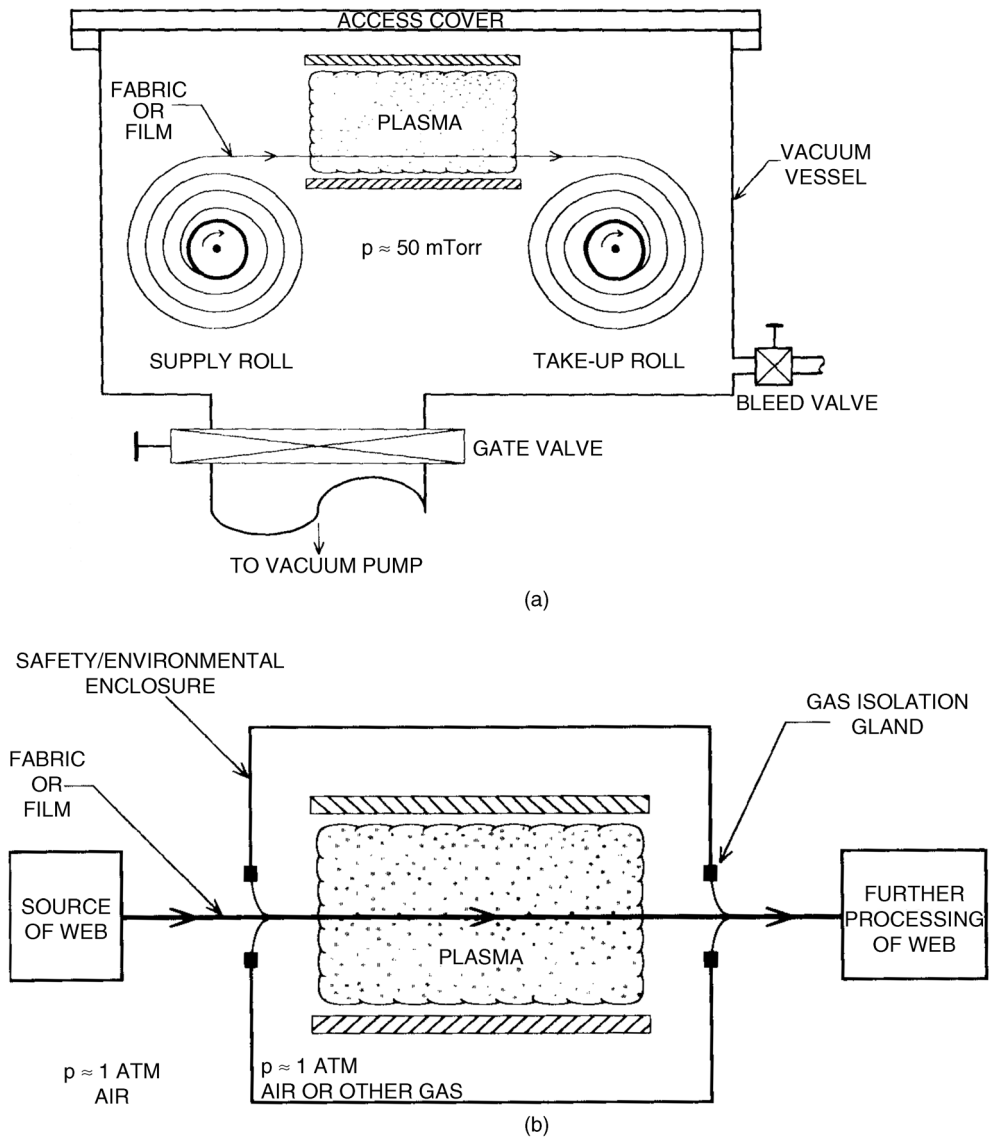
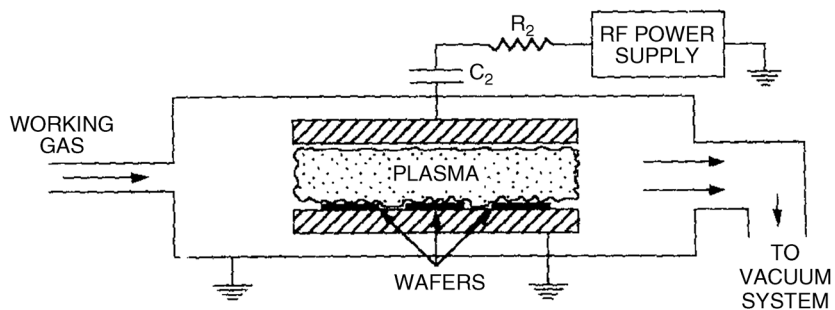
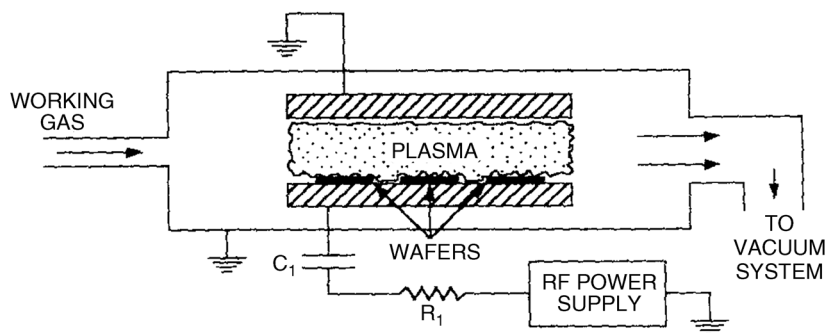


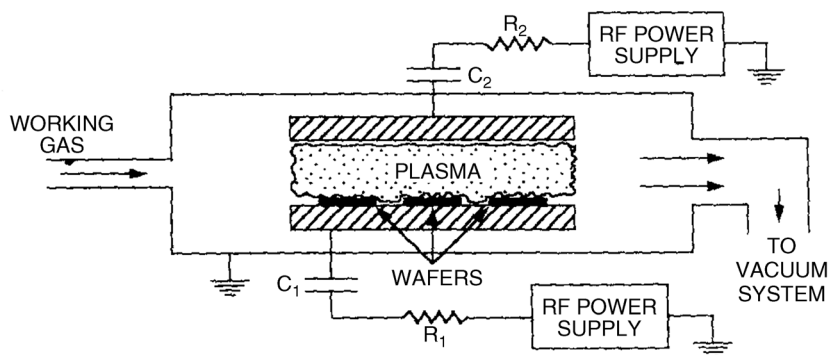
Figure 1.18 Industrial plasma modification of textile surfaces. Plasma reactor configurations for (a) low-pressure batch processing and (b) continuous processing at atmospheric pressure. Adapted with permission from Ref. [122]; © 1995, Institute of Physics Publishing.



(a) PLASMA ETCHING CONFIGURATION



(b) REACTIVE ION ETCHING CONFIGURATION



(c) TRIODE ETCHING CONFIGURATION

Figure 1.19 Industrial plasma etching of wafers. Plasma reactor configurations for low-pressure processing. Adapted with permission from Ref. [122]; © 1995, Institute of Physics Publishing.

References

- 1 Debye, P. (1929) *Polar Molecules*, Chemical Catalog Co., New York.
- 2 Debye, P. (1935) Molecular rotation in liquids. *Phys. Z.*, **36**, 100.
- 3 Parodi, F. (1996) Physics and chemistry of microwave processing, Chapter 19, in *Comprehensive Polymer Science, Second Supplement* (eds S.L. Aggarwal and S. Russo), Pergamon, Oxford, p. 669.
- 4 (a) Havriliak, S. and Negami, S. (1966) A complex plane analysis of α -dispersions in some polymer systems. *J. Polym. Sci. C*, **14**, 99; (b) Havriliak, S. and Negami, S. (1967) A complex plane representation of dielectric and mechanical relaxation processes in some polymers. *Polymer*, **8**, 161.
- 5 Cole, K.S. and Cole, R.H. (1941) Dispersion and absorption in dielectrics. *J. Chem. Phys.*, **9**, 341.
- 6 Metaxas, A.C. and Meredith, R.J. (1983) *Industrial Microwave Heating*, Peregrinus, London.
- 7 Brandrup, J. and Immergut, E.H. (eds) (1989) *Polymer Handbook*, 3rd edn, John Wiley, New York.
- 8 Huang, H.T. (1976) Temperature control in a microwave resonant cavity system for rapid heating of nylon monofilament. *J. Microwave Power Electromagn. Energy*, **11**, 305.
- 9 Bogdal, D., Penczek, P., Pielichowski, J., and Prociak, A. (2003) Microwave-assisted synthesis, crosslinking, and processing of polymeric materials. *Adv. Polym. Sci.*, **163**, 193.
- 10 Wiesbrock, F., Hoogenboom, R., and Schubert, U. (2004) Microwave-assisted polymer synthesis: state-of-the-art and future perspectives. *Macromol. Rapid Commun.*, **25**, 1739.
- 11 Zhang, D., Crivello, J.V., and Stoffer, J.O. (2004) Polymerizations of epoxides with microwave energy. *J. Polym. Sci., Part B: Polym. Phys.*, **42**, 4230.
- 12 Loupy, A. (ed.) (2006) *Microwaves in Organic Synthesis*, 2nd edn, Wiley-VCH, Weinheim.
- 13 Kappe, C.O. and Stadler, A. (2005) *Microwaves in Organic and Medicinal Chemistry*, Wiley-VCH, Weinheim.
- 14 Kappe, C.O. (2004) Controlled heating with microwaves in modern organic synthesis. *Angew. Chem. Int. Ed.*, **43**, 6250.
- 15 Man, A.K. and Shahidan, R. (2007) Microwave-assisted chemical reactions. *J. Macromol. Sci., Pure Appl. Chem.*, **44**, 651.
- 16 Bogdal, D. and Prociak, A. (2007) *Microwave-Enhanced Polymer Chemistry and Technology*, Blackwell Publishing, Ames, IA, USA.
- 17 Bogdal, D. and Matras, K. (2006) Polymer Chemistry under the Action of Microwave Irradiation, in *Microwaves in Organic Synthesis* (ed. A. Loupy), 2nd edn, Wiley-VCH, Weinheim, Ch. 14.
- 18 Bogdal, D. (2005) *Microwave-Assisted Organic Synthesis: One Hundred Reaction Procedures*, Elsevier, Amsterdam.
- 19 Zong, L., Zhou, S., Sgriccia, N., Hawley, M.C., and Kempe, L.C. (2003) A Review of microwave-assisted polymer chemistry (MAPC). *J. Microwave Power Electromagn. Energy*, **38**, 49.
- 20 Mingos, D.M.P. and Baghurst, D.R. (1991) Applications of microwave dielectric heating effects to synthetic problems in chemistry. *Chem. Soc. Rev.*, **20**, 1.
- 21 Elias, H.-G. (2005) Macromolecules, in *Chemical Structures and Syntheses*, vol. 1, Wiley-VCH, Weinheim.
- 22 Mishra, M.K. and Yagci, Y. (eds) (1998) *Handbook of Radical Vinyl Polymerization*, Dekker, New York.
- 23 Cowie, J.M.G. and Arrighi, V. (2007) *Polymers, Chemistry and Physics of Modern Materials*, 3rd edn, CRC Press, Boca Raton.
- 24 Moad, G. and Solomon, D.H. (2005) *The Chemistry of Free Radical Polymerization*, 2nd edn, Elsevier Science, Oxford.
- 25 Palacios, J.J. and Valverde, C. (1996) Microwave initiated emulsion polymerization of styrene: reaction conditions. *New Polym. Mater.*, **5**, 93.
- 26 Hoogenboom, R., Wiesbrock, F., Huang, H., Leenen, M.A.M., Thijs, H.M.L., van Nispen, S.F.G.M., van der Loop, M., Fustin, C.-A., Jonas, A.M., Gohy, J.-F., and Schubert, U.S. (2006) Microwave-assisted ring-opening cationic polymerization of

- 2-oxazolines: a powerful method for the synthesis of amphiphilic triblock terpolymers. *Macromolecules*, **39**, 4719.
- 27 Fang, X., Hutcheon, R., and Scola, D.A. (2000) Microwave syntheses of Poly (ϵ -caprolactam-co- ϵ -caprolactone). *J. Polym. Sci., Part A: Polym. Chem.*, **38**, 1379.
 - 28 Stoffer, J.O., Zhang, D., and Crivello, J.V. (1999) Cationic polymerizations of epoxides using microwave energy. *Polym. Mater. Sci. Eng.*, **81**, 118.
 - 29 van Dijk, M., Mustafa, K., Dechesne, A.C., van Nostrum, C.F., Hennink, W.E., Rijkers, D.T.S., and Liskamp, R.M.L. (2007) Synthesis of peptide-based polymers by microwave-assisted cycloaddition by backbone polymerization. *Biomacromolecules*, **8**, 327.
 - 30 Lewis, D.A., Summers, J.D., Ward, T.C., and McGrath, E.J. (1992) Accelerated imidization reactions using microwave radiation. *J. Polym. Sci., Part A: Polym. Chem.*, **30**, 1647.
 - 31 Mijovic, J., Corso, W.V., Nicolais, L., and d'Ambrosio, G. (1998) *In situ* real-time study of crosslinking kinetics in thermal and microwave fields. *Polym. Adv. Technol.*, **9**, 231.
 - 32 Ludlow-Palafox, C. and Chase, H.A. (2001) Microwave-induced pyrolysis of plastic wastes. *Ind. Eng. Chem. Res.*, **40**, 4749.
 - 33 Danko, G.A., Silbergliitt, R., Colombo, P., Pippel, E., and Woltersdorf, J. (2000) Comparison of microwave hybrid and conventional heating of preceramic polymers to form silicon carbide and silicon oxycarbide ceramics. *J. Am. Ceram. Soc.*, **83**, 1617.
 - 34 Klun, U. and Krzan, A. (2000) Rapid microwave induced depolymerization of polyamide-6. *Polymer*, **41** (11), 4361.
 - 35 Krzan, A. (1998) Microwave irradiation as an energy source in poly(ethylene terephthalate) solvolysis. *J. Appl. Polym. Sci.*, **69**, 1115.
 - 36 Kleps, T., Piaskiewicz, M., and Parasiewicz, W. (2000) The use of thermogravimetry in the study of rubber devulcanization. *J. Therm. Anal. Calorim.*, **60**, 271.
 - 37 Engelhart, W.G. (1997) Microwave hydrolysis of proteins and peptides for amino acid analysis, in *Microwave-Enhanced Chemistry* (eds H.M. Kingston and S.J. Haswell), American Chemical Society, Washington DC, USA, Ch. 13.
 - 38 Galema, S.A. (1997) Microwave chemistry. *Chem. Soc. Rev.*, **26**, 233.
 - 39 Larhed, M. and Halberg, A. (2001) Microwave-assisted high-speed chemistry: a new technique in drug discovery. *Drug Disc. Today*, **6**, 406.
 - 40 (a) Stadler, A. and Kappe, C.O. (2001) High-speed couplings and cleavages in microwave-heated, solid-phase reactions at high temperatures. *Eur. J. Org. Chem.*, **919**; (b) Stadler, A. and Kappe, C.O. (2001) The effect of microwave irradiation on carbodiimide-mediated esterifications on solid support. *Tetrahedron*, **57**, 3915.
 - 41 Lin, M.J. and Sun, C.M. (2003) Microwave-assisted traceless synthesis of thiohydantoin. *Tetrahedron Lett.*, **44**, 8739.
 - 42 Mallon, F.K. and Ray, W.H. (1998) Enhancement of solid-state polymerization with microwave energy. *J. Appl. Polym. Sci.*, **69**, 1203.
 - 43 de la Hoz, A., Diaz-Ortiz, A., and Moreno, A. (2005) Microwave in organic synthesis. thermal and non-thermal microwave effects. *Chem. Soc. Rev.*, **34**, 164.
 - 44 Perreux, L. and Loupy, A. (2006) Non-thermal Effects of Microwaves in Organic Synthesis, in *Microwaves in Organic Synthesis* (ed. A. Loupy), 2nd edn, Wiley-VCH, Weinheim, Ch. 3.
 - 45 Biederman, H. (ed.) (2004) *Plasma Polymer Films*, Imperial College Press, London.
 - 46 Bradley, A.P. and Hammes, J.P. (1963) Electrical properties of thin organic films. *J. Electrochem. Soc.*, **10**, 15.
 - 47 Favia, P. (2004) Plasma Deposition of Fluoropolymer Films in Different Glow Discharge Regimes, in *Plasma Polymer Films* (ed. H. Biederman), Imperial College Press, London, Ch. 2.
 - 48 Hamblyn, S.M.L. and Reuben, B.G. (1975) Use of radio-frequency plasma in chemical synthesis. *Adv. Inorg. Radio Chem.*, **17**, 89.
 - 49 Yasuda, H. (1985) *Plasma Polymerization*, Academic Press, Orlando.
 - 50 Inagaki, N. (1995) *Plasma Surface Modification and Plasma Polymerization*, Technomic Publ. AG, Basel.
 - 51 d'Agostino, R., Favia, P., Oehr, C., and Wertheimer, M.R. (eds) (2005) *Plasma*

- Processes and Polymers*, Wiley-VCH, Weinheim.
- 52 Friedrich, J.F., Mix, R., and Kühn, G. (2005) Polymer Surface Modification with Monotype Functional Groups of Different Type and Density, in *Plasma Processes and Polymers* (eds R. d'Agostino, P. Favia, C. Oehr, M.R. Wertheimer), Wiley-VCH, Weinheim, p. 3.
 - 53 Friedrich, J.F., Mix, R., Schulze, R.D., and Kühn, G. (2005) Contribution of chemical interaction to the adhesion between metals and functional groups of different (Mono-) type and density at polymer surfaces, in *Adhesion* (ed. W. Possart), Wiley-VCH, Weinheim, Ch. 18, p. 265.
 - 54 Legeay, G. and Poncin-Epaillard, F. (2005) Surface engineering by coating of hydrophilic layers: bioadhesion and biocontamination, in *Adhesion* (ed. W. Possart), Wiley-VCH, Weinheim, Ch. 12, p. 175.
 - 55 Siffer, F., Schultz, J., and Roucoules, V. (2005) Alkene pulsed plasma functionalized surfaces: an interfacial Diels–Alder study, in *Adhesion* (ed. W. Possart), Wiley-VCH, Weinheim, Ch. 19, p. 289.
 - 56 Biederman, H. and Osada, Y. (1992) *Plasma Polymerization Processes*, Elsevier, Amsterdam.
 - 57 Rossmann, K. (1956) Improvement of bonding properties of polyethylene. *J. Polym. Sci.*, **19**, 141.
 - 58 Strobel, M., Lyons, C.S., and Mittal, K.L. (eds) (1994) *Plasma Surface Modification of Polymers*, VSP Press, Zeist, Netherlands.
 - 59 Wertheimer, M.R., Martinu, L., Klemberg-Sapieha, J.E., and Czeremuszkin, G. (1999) Plasma treatment of polymers to improve adhesion, in *Adhesion Promotion Techniques, Technological Applications* (eds K.L. Mittal and A. Pizzi), Dekker, New York., Ch. 5.
 - 60 Hegemann, D., Hossain, M.M., Körner, E., and Balazs, D.J. (2007) A Macroscopic Description of Plasma Polymerization, in *Proceedings, 10th International Conference on Plasma Surface Engineering, Garmisch-Partenkirchen, 2006* (eds A. Cavaleiro, R. Grün, U. Helmersson, W. Möller, J. Musil, and C. Oehr), Wiley-VCH, Weinheim, p. 229.
 - 61 Hippler, R., Pfau, S., Schmidt, M., and Schoenbach, K.H. (eds) (2001) *Low Temperature Plasmas, Fundamental Aspects and Applications*, Wiley-VCH, Weinheim.
 - 62 Hippler, R., Kersten, H., Schmidt, M., and Schoenbach, K.H. (eds) (2008) *Low Temperature Plasmas, Fundamentals, Technologies and Techniques*, Wiley-VCH, Weinheim.
 - 63 *Plasma Processes and Polymers* (2013) vol. **10**, Wiley-VCH. Print-ISSN: 1612-8850; Online ISSN: 1612-8869.
 - 64 *Plasmas and Polymers*. Springer. Print-ISSN: 1084-0184 (discontinued).
 - 65 Christophorou, L.G. (1971) *Atomic and Molecular Radiation Physics*, Wiley-Interscience, London.
 - 66 d'Agostino, R., Camarossa, F., Fracasse, F., and Illuzzi, F. (1990) Plasma Polymerization of Fluorocarbons, in *Plasma Deposition, Treatment and Etching of Polymers* (ed. R. d'Agostino), Academic Press, Boston, Ch. 2.
 - 67 Kogoma, M. (2004) Application of Atmospheric Pressure Discharge for Plasma Polymer Processes, in *Plasma Polymer Films* (ed. H. Biederman), Imperial College Press, London, Ch. 8.
 - 68 Becker, K.H., Kogelschatz, U., Schoenbach, K.H., and Barker, R.J. (eds) (2004) *Non-Equilibrium Plasmas at Atmospheric Pressure*, Institute of Physics Publ., Bristol.
 - 69 Hopfe, V. and Scheel, D.W. (2007) Atmospheric Pressure Plasmas for Wide-Area Thin-Film Deposition and Etching, in *Proceedings 10th International Conference on Plasma Surface Engineering, Garmisch-Partenkirchen, 2006* (eds A. Cavaleiro, R. Grün, U. Helmersson, W. Möller, J. Musil, and C. Oehr), Wiley-VCH, Weinheim, p. 253.
 - 70 d'Agostino, R. (ed.) (1990) *Plasma Deposition, Treatment and Etching of Polymers*, Academic Press, Boston.
 - 71 Manos, D.M. and Flamm, D.L. (eds) (1989) *Plasma Etching – An Introduction*, Academic Press, Boston.
 - 72 Mucha, J.A. and Hess, D.W. (1983) Plasma etching, in *Introduction to Microlithography* (eds L.F. Thompson, C.G., Willson, and M.J. Bowden), American Chemical Society, Washington, Ch. 5.

- 73 Kay, E. (1982) Reactive ion etching and related polymerization processes, in *Methods and Materials in Microelectronic Technology* (ed. J. Bargon), Plenum Press, New York.
- 74 Richter, H.H. and Wolff, A. (2001) Plasma Etching in Microelectronics, in *Low Temperature Plasmas, Fundamental Aspects and Applications* (eds R. Hippler, S. Pfau, M. Schmidt, and K.H. Schoenbach), Wiley-VCH, Weinheim, Ch. 18.
- 75 Richter, H.H., Marschmeyer, S., and Wolff, A. (2008) Plasma Etching in Microelectronics, in *Low Temperature Plasmas, Fundamentals, Technologies and Techniques* (eds R. Hippler, H. Kersten, M. Schmidt, and K.H. Schoenbach), Wiley-VCH, Weinheim, Ch. 25.
- 76 Cavaleiro, A., Grün, R., Helmersson, U., Möller, W., Musil, J., and Oehr, C. (eds) (2007) Plasma surface engineering, in *Proceedings 10th International Conference on Plasma Surface Engineering, Garmisch-Partenkirchen, 2006*, Wiley-VCH, Weinheim.
- 77 Meichsner, J. (2001) Low Temperature Plasmas for Polymer Surface Modification, in *Low Temperature Plasmas, Fundamental Aspects and Applications* (eds R. Hippler, S. Pfau, M. Schmidt, and K.H. Schoenbach), Wiley-VCH, Weinheim, Ch. 19.
- 78 Liston, E.M. (1993) Plasmas and surfaces – a practical approach to good composites, in *The Interfacial Interaction in Polymeric Composites* (ed. G. Akozali), Kluwer, Dordrecht, vol. 230, Ch. 10.
- 79 Kawakami, M., Yamashita, Y., Iwamoto, M., and Kagawa, S. (1984) Modification of gas permeabilities of polymer membranes by plasma coating. *J. Membrane Sci.*, **19**, 249.
- 80 Morosoff, N. (1990) An Introduction to Plasma Polymerization, in *Plasma Deposition, Treatment and Etching of Polymers* (ed. R. d'Agostino), Academic Press, Boston, Ch. 1.
- 81 Havriliak, S. and Havriliak, S.J. (1997) *Dielectric and Mechanical Relaxation in Materials: Analysis, Interpretation, and Application to Polymers*, Hanser, München.
- 82 Riande, E. and Diaz-Caleja, R. (2004) *Broadband Dielectric Spectroscopy*, Dekker, New York.
- 83 Kremer, F. and Schönhals, A. (eds) (2003) *Broadband Dielectric Spectroscopy*, Springer, Berlin.
- 84 Runt, J.P. and Fitzgerald, J.J. (eds) (1997) *Dielectric Spectroscopy of Polymeric Materials, Fundamentals and Applications*, American Chemical Society, Washington, DC, USA.
- 85 McCrum, N.G., Read, B.E., and Williams, G. (1991) *Anelastic and Dielectric Effects in Polymer Solids*, Dover, New York.
- 86 Schönhals, A. (2004) Dielectric Properties of Amorphous Polymers, in *Broadband Dielectric Spectroscopy* (eds E. Riande and R. Diaz-Caleja), Dekker, New York, Ch. 3.
- 87 Asami, K. (2002) Characterization of heterogeneous systems by dielectric spectroscopy. *Prog. Polym. Sci.*, **27**, 1617.
- 88 Kremer, F. and Schönhals, A. (2003) Broadband Dielectric Measurement Techniques (10^{-6} Hz to 10^{12} Hz), in *Broadband Dielectric Spectroscopy* (eds F. Kremer and A. Schönhals), Springer, Berlin, Ch. 2.
- 89 Feldman, Y.D., Zuev, Y.F., Polygalov, E.A., and Fedotov, V.D. (1992) Time domain dielectric spectroscopy. A new effective tool for physical chemistry investigations. *Colloid Polym. Sci.*, **270**, 768.
- 90 Cole, R.H., Berberian, J.G., Mashimo, S., Chrysikos, G., Burns, A., and Tombari, E. (1989) Time domain reflection methods for dielectric measurements to 10 GHz. *J. Appl. Phys.*, **66**, 793.
- 91 Kremer, F., Hofmann, A., and Fischer, E. W. (1992) Broadband dielectric measurements on the α - and β -relaxation of polymers – a test of mode coupling. *Am. Chem. Soc., Polym. Prepr.*, **33**, 96.
- 92 Pethrick, R.A. and Hayward, D. (2002) Real time dielectric relaxation studies of dynamic polymeric systems. *Prog. Polym. Sci.*, **27**, 1983.
- 93 van den Berg, O., Sengers, W.G.F., Jager, W.F., Picken, S.J., and Wübbenhorst, M. (2004) Dielectric and fluorescent probes to investigate glass transition, melt, and crystallization in polyolefins. *Macromolecules*, **37**, 2460.

- 94 Kessairi, K., Napolitano, S., Cappacioli, S., Rolla, P., and Wübbenhorst, M. (2007) Molecular dynamics of atactic poly (propylene) investigated by broadband dielectric spectroscopy. *Macromolecules*, **40**, 1786.
- 95 Mie, W.N., Kohli, M., Prohofsky, E.W., and Van Zandt, L.L. (1981) Acoustic modes and nonbonded interactions of the double helix. *Biopolymers*, **20**, 833.
- 96 Gabriel, C., Grant, E.H., Tata, R., Brown, P. R., Gestblom, B., and Noreland, E. (1987) Microwave absorption in aqueous solutions of DNA. *Nature*, **328**, 145.
- 97 Bigio, I.J., Gosnet, T.R., Mukherjee, P., and Saffer, J.D. (1993) Microwave absorption spectroscopy of DNA. *Biopolymers*, **33**, 147.
- 98 Edwards, G.S., Davis, C.C., Saffer, J.D., and Swicord, M.L. (1984) Resonant microwave absorption of selected DNA molecules. *Phys. Rev. Lett.*, **53**, 1284.
- 99 Infelta, P.P., de Haas, M.P., and Warman, J.M. (1977) The study of the transient conductivity of pulse irradiated dielectric liquids on a nanosecond timescale using microwaves. *Radiat. Phys. Chem.*, **10**, 353.
- 100 Warman, J.M., de Haas, M.P., Pichat, P., Koster, T.M.P., van der Zouwen-Assink, E. A., Mackor, A., and Cooper, R. (1991) Electronic processes in semiconductor materials studied by nanosecond time-resolved microwave conductivity. *Radiat. Phys. Chem.*, **37**, 433.
- 101 Nespurek, S., Herden, V., Kunst, M., and Schnabel, W. (2000) Microwave photoconductivity and polaron formation in poly(methylphenyl silylene). *Synth. Met.*, **109**, 309.
- 102 Prins, P., Grozema, F.C., Schins, J.M., Patil, S., Scherf, U., and Siebbeles, L.D.A. (2006) High intrachain hole mobility on molecular wires of ladder type poly(*p*-phenylenes). *Phys. Rev. Lett.*, **96**, 146601.
- 103 Prins, P., Grozema, F.C., and Siebbeles, L.D.A. (2006) Efficient charge transport along phenylene-vinylene molecular wires. *J. Phys. Chem. B*, **110**, 14659.
- 104 Prins, P., Grozema, F.C., Schins, J.M., and Siebbeles, L.D.A. (2006) Frequency dependent mobility of charge carriers along polymer chains with finite length. *Phys. Status Solidi B*, **243**, 382.
- 105 Pastol, Y., Arjavalingam, G., Halbout, J.-M., and Kopcsay, G.V. (1989) Coherent broadband microwave spectroscopy using picosecond optoelectronic antennas. *Appl. Phys. Lett.*, **54**, 307.
- 106 Arjavalingam, G., Theophilou, N., Pastol, Y., Kopcsay, G.V., and Angelopoulos, M. (1990) Anisotropic conductivity in stretch oriented polymers measured with coherent microwave transient spectroscopy. *J. Chem. Phys.*, **93**, 6.
- 107 Zoughi, R. (2000) *Microwave Non-Destructive Testing and Evaluation*, Kluwer Academic Publ., Dordrecht.
- 108 Zoughi, R. (1995) Microwave and millimeter wave nondestructive testing: a succinct introduction. *Res. Nondestr. Eval.*, **7**, 71.
- 109 Diener, L. (1995) Microwave near-field imaging with open-ended waveguide – comparison with other techniques of non-destructive testing. *Res. Nondestr. Eval.*, **7**, 137.
- 110 Diener, L. and Busse, G. (1996) Non-destructive quality and process control in injection moulding polymer manufacture with microwaves. *Mater. Sci. Forum*, **210-213**, 665.
- 111 Green, R.E., Djordevic, B.B., and Hentschel, M.P. (eds) (2003) Nondestructive characterization of materials X, in *Proceedings of the 11th International Symposium, Berlin 2002*, Springer, Berlin.
- 112 Hinken, J.H. and Beilken, D. (2005) Microwave defectoscopy with extended eddy current system. *Online J. Nondestruct. Test.*, **NDT.net 10**, October. Available at: <http://www.ndt.net/v10n09.htm>.
- 113 Steegmüller, R., Diener, L., and Busse, G. (1999) Microwave characterization of glass fiber reinforced polymers with a multi-detector waveguide. *Progr. Quantit. Nondestr. Eval.*, **18**, 555.
- 114 Liu, J.M. (2003) Characterization of Layered Dielectric Composites by Radar Techniques, in *Proceedings of the 11th International Symposium, Berlin 2002* (eds R.E. Green, B.B. Djordevic, and M.P. Hentschel), Springer, Berlin, p. 291.
- 115 Predak, S., Solodov, I.Y., Busse, G., Bister, V.H., Vöhringer, M.C., Haberstroh, E., and Ehbing, H. (2006)

- Fiber orientation measurement on short fiber reinforced PUR-RIM components: combination of nondestructive testing methods for optimization of simulation and production processes. *Tech. Mess.*, **73**, 617.
- 116** Predak, S., Ringer, T., Aicher, S., and Busse, G. (2003) Inspection of Dielectric Materials with Microwaves, in *Proceedings of the 11th International Symposium, Berlin 2002* (eds R.E. Green, B.B. Djordevic, and M.P. Hentschel), Springer, Berlin, p. 281.
- 117** Otto, J., Pannert, W., and Hald, M. (2003) Detection of Hidden Corrosion under Paint, in *Proceedings of the 11th International Symposium, Berlin 2002* (eds R.E. Green, B.B. Djordevic, and M.P. Hentschel), Springer, Berlin, p. 297.
- 118** Han, H.C. and Mansueto, E.S. (1995) Thin film inspection with millimeter-wave reflectometer. *Res. Nondestr. Eval.*, **7**, 89.
- 119** Han, H.C. and Mansueto, E.S. (1997) Thick measurement for thin films and coatings using millimeter waves. *Res. Nondestr. Eval.*, **9**, 97.
- 120** Krieger, B. (1992) Vulcanization of rubber, a resounding success for microwave processing. *Polym. Mater. Sci. Eng.*, **66**, 339.
- 121** Parodi, F. (2013) Novel Specialty Microwave Heating Susceptors for the Fast UHF Vulcanization of White and Colored Rubber Compounds, Technical Brochure. Available at: http://www.fpchem.com/fap_6a2-en.html.
- 122** Reece Roth, J. (1995) Industrial Plasma Engineering, vol. 1, *Applications to Nonthermal Plasma Processing*, vol. 2, *Principles*. IOP Publishing, Bristol (reprinted 2001).
- 123** Wertheimer, M.R., Fozza, A.C., and Hollander, A. (1999) Industrial processing of polymers by low-pressure plasmas: the role of VUV radiation. *Nucl. Instr. Meth., Phys. Res. B*, **151**, 65.
- 124** Wertheimer, M.R., Martinu, L., and Liston, E.M. (1996) Plasma sources for polymer surface treatment, in *Handbook of Thin Film Process Technology* (eds D.A. Glocker and S.I. Shah), IOP Publishing, Bristol.